arXiv:2507.20804v2 [cs.AI] 10 Mar 2026

MMGraphRAG: Bridging Vision and Language with Interpretable Multimodal Knowledge Graphs

Xueyao Wan
Harbin Institute of Technology
China
1185909349@qq.com

Hang Yu
Nanyang Technological University
Singapore
hang023@e.ntu.edu.sg

Abstract

Large Language Models (LLMs) excel at natural language generation but often suffer from hallucinations due to their static parametric nature. Retrieval-Augmented Generation (RAG) mitigates this limitation by incorporating external knowledge, while GraphRAG further enhances reasoning by leveraging knowledge graphs (KGs).

One limitation, however, is that methods based on GraphRAG are still limited to textual data because of the difficulty of constructing a fine-grained multimodal KG (MMKG). All existing text–image fusion methods, including mapping images and texts into a shared embedding space, image captioning, and joint text–image extraction, rely heavily on task-specific training and suffer from limited generalization. More importantly, they fail to preserve the structural knowledge of visual content or capture the structure of knowledge and reasoning paths between modalities. Thus, they cannot construct an MMKG that incorporates both image and textual entities.

To address these limitations, we propose MMGraphRAG, which refines visual content through scene graphs and integrates it with text-based knowledge graphs to construct an MMKG via a novel cross-modal fusion approach. It employs the SpecLink method, which leverages spectral clustering-based candidate entities generation method to achieve accurate cross-modal entity linking and retrieves context along reasoning paths to guide the generative process. Due to the lack of benchmarks, we also release the CMEL dataset, which is designed for fine-grained multi-entity alignment in complex multimodal scenarios. The experiments on this dataset validate the effectiveness of the SpecLink method in complex multimodal scenarios. To evaluate MMGraphRAG, we conduct experiments on the DocBench and MMLongBench datasets. Results show that MMGraphRAG achieves state-of-the-art performance, demonstrating strong domain adaptability and multimodal information processing capability.

CCS Concepts

• **Information systems → Question answering**; **Content analysis and feature selection**.

Keywords

GraphRAG, Cross-Modal Entity Linking, Scene Graph

1 Introduction

Large Language Models (LLMs) have advanced in natural language generation, yet hallucination—factual inconsistency—remains a major limitation[21, 35, 45]. Due to their static parametric nature, LLMs cannot promptly integrate specialized and up-to-date data, causing incomplete or inaccurate knowledge in professional fields[9, 12, 20, 62]. Retrieval-Augmented generation (RAG) mitigates this by incorporating external knowledge bases, retrieving relevant documents to enrich the generative process with up-to-date context, thereby reducing hallucinations[28]. To improve the performance on complex QA tasks, researchers have integrated knowledge graphs (KGs) to enhance the reasoning capabilities and interpretability of RAG systems, such as GraphRAG, which integrates local and global knowledge by constructing entity KGs and community summaries[15]. However, methods based on GraphRAG are still limited to textual data because of the difficulty of constructing proper multimodal KG (MMKG). Text-only GraphRAG methods cannot fully exploit visual information, leading to incomplete retrieval results[32], since real-world information often co-exists in multimodal forms such as text, images, and tables.

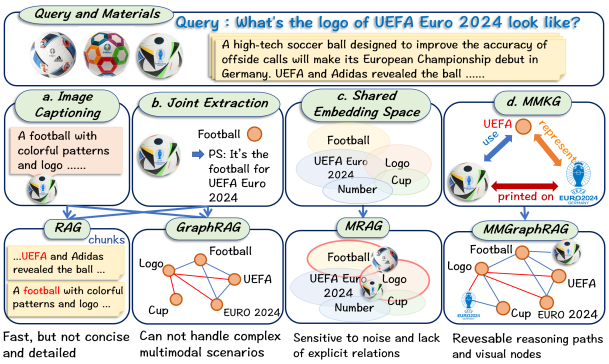

Figure 1: Comparison of Image-Text Fusion Methods. Prior methods struggle with accurate visual reasoning: (a) Captioning-based methods linearize the image into a single text description, irretrievably losing fine-grained details. (b) Joint Extraction depends on precise annotations and fails in complex scenarios where key visual entities, like the logo itself, are unlabeled. (c) Shared Embedding MRAG struggles to isolate specific attributes from a flattened, implicit vector. In contrast, (d) our MMGraphRAG constructs a Multimodal Knowledge Graph, representing the logo and football as explicit visual nodes linked to text. This preserves the essential knowledge structure, enabling precise and interpretable answers.

To bridge this gap, we propose MMGraphRAG framework with a creative and zero-shot construction method of fine-grained MMKG. To facilitate the MMGraphRAG system, the MMKG should construct KG for the image modality and enable fusion connections across image–text modalities which remains graph structure. Our

method achieves these by utilizing scene graphs and designing a novel cross modal entity linking (CMEL) method called SpecLink, ensuring that image information is preserved in the MMKG as entities and integrated with textual entities via high-quality links. All existing alternative multimodal fusion approaches, such as mapping images and text into a shared embedding space[11, 16, 34, 67], image captioning[56, 70], and image-text joint extraction[54, 72], fail to realize these key points and require large amounts of domain-specific training. Figure 1 presents a comparison of these multimodal fusion methods. As shown, the successful construction of the MMKG retains knowledge structure and reasoning paths, allowing the MMGraphRAG approach to deliver more comprehensive and accurate results, thereby mitigating hallucinations.

The key point of constructing MMKG is CMEL task, which enables the establishment of connections between entities from different modalities[65]. However, research in this area remains in its early stage, and there is a lack of benchmarks to evaluate the task comprehensively. To address this, we build and release the CMEL dataset. Motivated by the challenges of accurate candidate selection in this task, we introduce the SpecLink method, which leverages spectral clustering to generate high-quality candidate entities for every visual entities, effectively enhancing the accuracy of the CMEL task. Finally, context is retrieved along multimodal reasoning paths within the MMKG to guide the generative process.

Evaluated on two challenging benchmarks, MMGraphRAG demonstrates significant superiority. On DocBench[73], it achieves 76.8% overall accuracy, far exceeding NaiveRAG (59.5%) and GraphRAG (52.3%). This advantage is especially pronounced in multimodal queries (88.7% accuracy), showcasing effective visual-textual integration. Similarly, on MMLongBench[42], MMGraphRAG establishes a new state of the art with 38.8% accuracy and a 34.1% F1 score, excelling in complex chart and figure reasoning. Crucially, our framework demonstrates exceptional robustness in identifying unanswerable questions, outperforming a leading multimodal RAG method by over sixfold (35.1% vs. 5.8%). This highlights the effectiveness of its explicit MMKG reasoning in mitigating hallucinations. Further ablation studies confirm that our spectral clustering-based fusion mechanism is critical, preventing the introduction of noise and substantially boosting performance over naive fusion methods. Overall, MMGraphRAG provides not only superior accuracy but also more reliable and interpretable reasoning paths.

Our main contributions are as follows:

(1) **MMGraphRAG framework:** We propose MMGraphRAG, which refines images into scene graphs and combines them with text-based KG to build a unified MMKG for cross-modal reasoning.
(2) **CMEL dataset:** We build and release the CMEL dataset, specifically designed for alignment between visual and textual entities, addressing the lack of benchmarks in this area.
(3) **SpecLink method:** We design a cross-modal entity alignment process, utilizing spectral clustering to efficiently generate candidate entities by integrating semantic and structural information, thereby enhancing the accuracy of the CMEL task.

2 Related Work

2.1 Image-Text Fusion Methods

Research on multimodal fusion as the upstream of RAG has mainly progressed along following directions. First, image captioning methods adopt encoder–decoder frameworks that translate images into textual descriptions, thereby "linearizing" visual semantics before retrieval or reasoning[56]. For example, while recent models incorporate scene graph encoding to better encode object relationships[70], the structural information remains only implicitly folded into the captioning model. The final output is still a free-form textual description, which discards the explicit knowledge structure and lack transparent reasoning paths.

Second, shared embedding space approaches align images and text in a joint vector space using large-scale contrastive pretraining, achieving robust zero-shot retrieval but sensitive to noise and also leading to semantic flattening[11, 16, 34, 67]. The specialization caused by training, along with noisy evidence in a shared embedding space, can mislead the model into confidently generating incorrect answers[43]. For instance, M3DocRAG achieves only 5.8% accuracy on questions with "unanswerable" ground truths, underscoring significant weaknesses in factual consistency [11]. Thus, the limitations of this method in structured reasoning, generalizability, and hallucination reduction call for further improvement.

Third, multimodal alignment with constraints leverages semantic priors to disambiguate entity linking across modalities, such as enforcing consistency between object regions and textual mentions[54], or constraining alignment through syntactic or semantic cues[72]. While such methods improve disambiguation, they rely on task-specific annotations or heuristics and thus suffer from limited generalizability. In contrast, our method explicitly integrates scene graphs into an MMKG by treating visual nodes as first-class entities and linking them to textual counterparts via CMEL. This enables structure-preserving retrieval and interpretable multimodal reasoning while directly utilizing visual information without semantic flattening.

2.2 MMKG Construction Paradigms: N-MMKG vs. A-MMKG

In the construction of Multimodal Knowledge Graphs (MMKGs), information can be integrated using two primary paradigms. The conventional attribute-centric MMKG (A-MMKG) approach treats visual and textual information as distinct modalities, where non-textual data is typically embedded as an entity's attribute. However, this method can lead to significant semantic loss, particularly when modeling intricate cross-modal relationships [30]. To address this limitation, our framework adopts a node-based MMKG (N-MMKG) paradigm as its foundation.

The distinction is best illustrated with a medical example. In an A-MMKG, a "Patient" entity might possess an attribute such as "has_scan: mri_001.jpg". This structure relegates the image to a passive descriptor, making it impossible to model a direct relationship from the MRI scan to a specific clinical finding. In contrast, the N-MMKG paradigm elevates the MRI scan to a standalone node. This allows for the explicit modeling of crucial, fine-grained relations, such as "mri_001.jpg shows evidence of Anomaly". The image is

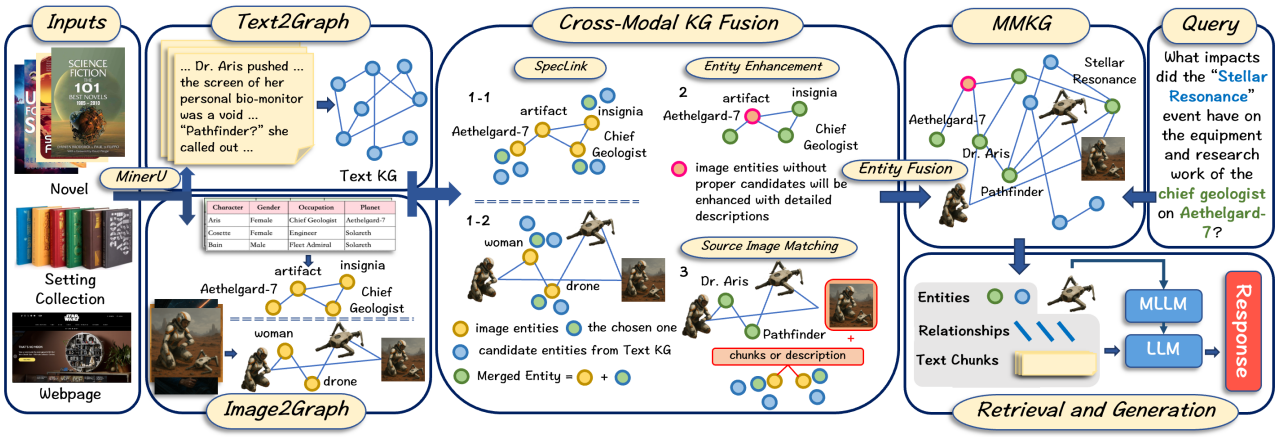

Figure 2: MMGraphRAG Framework Overview. The framework begins by parsing sources like novels and webpages, creating parallel knowledge graphs through Text2Graph for text and Image2Graph for visual content. The central Cross-Modal KG Fusion module then unifies these graphs by intelligently linking entities; for example, it uses SpecLink method to align the textual mention of the "Dr. Aris" with the corresponding "woman" in the image. This process yields a cohesive MMKG. Finally, during the Retrieval and Generation stage, this MMKG provides structured, cross-modal context to an MLLM/LLM system, enabling it to answer complex queries with accurate, well-supported responses.

no longer just a data point but an active component of the graph's relational structure.

This node-based architecture is fundamentally better suited for our framework because it preserves the rich, cross-modal semantics required for complex reasoning. It also significantly enhances flexibility and scalability. By design, new modalities can be seamlessly integrated as independent nodes without requiring structural modifications to the existing graph, ensuring a more robust and extensible knowledge foundation.

2.3 Entity Linking

Entity Linking (EL) has evolved from text-only methods to Multimodal Entity Linking (MEL), and more recently to Cross-Modal Entity Linking (CMEL), which supports cross-modal reasoning[5]. Traditional EL methods associate textual entities with their corresponding entries in a knowledge base, but overlook non-textual information [46, 47]. MEL extends EL by incorporating visual information as auxiliary attributes to enhance alignment between entities and knowledge base entries [17, 38, 49]. However, MEL does not establish cross-modal relations beyond these auxiliary associations, thereby limiting genuine cross-modal interaction.

CMEL goes further by treating visual content as entities—aligning visual entities with their textual counterparts—to construct MMKGs and facilitate explicit cross-modal inference [65]. Research on CMEL remains in its early stages, lacking a unified theoretical framework and robust evaluation protocols. The MATE benchmark is introduced to assess CMEL performance, but its synthetic 3D scenes fall short in capturing the complexity and diversity of real-world images [5]. To bridge this gap, we construct a CMEL dataset featuring greater real-world complexity and propose SpecLink method to drive further advances in CMEL research.

3 Methodology

To facilitate effective cross-modal information fusion and reasoning, we propose MMGraphRAG, a novel framework, which extends the conventional GraphRAG pipeline by incorporating dedicated mechanisms for visual modality processing and integration. It enables the joint construction of MMKGs from textual and visual inputs, thereby supporting retrieval and generation based on multimodal data.

3.1 MMGraphRAG Framework

The overall architecture of the proposed MMGraphRAG framework is illustrated in Figure 2. It consists of three stages: Indexing, Retrieval, and Generation. In contrast to query-based methods, where a temporary graph is constructed during the retrieval phase based on the query information and the database[6], the MMGraphRAG framework provides a more scalable solution. The MMKG built by MMGraphRAG can function as an independent knowledge base. Once created, it can be used across various queries without requiring re-building, making it ideal for large-scale question-answering scenarios.

The goal of the indexing stage is to transform raw multimodal data (text and images) into a structured MMKG. This stage comprises three sub-modules:

- **Preprocessing Module:** This module parses input documents using tools such as *MinerU* [57], extracting and separating textual and visual content. The data are then standardized for downstream processing.
- **Single-Modal Processing Module:** For textual inputs, document chunking and entity extraction are performed to construct a text-based KG. For visual inputs, image segmentation, scene graph construction, and entity alignment are applied to generate an image-based KG.

- **Cross-Modal Fusion Module:** This module employs our SpecLink method to identify candidate entity pairs for fusion. It then performs cross-modal entity linking to merge text-based KG and image-based KG into a unified MMKG.

The retrieval stage extends the traditional GraphRAG by incorporating image-based information, enhancing the retrieved entities and relations with visual data. In the generation stage, a hybrid approach is used, where the LLM handles the logical flow and textual response generation, while the MLLM focuses on processing the image retrieval results. This approach improves upon the GraphRAG method by adding image information to the retrieval process, allowing for more comprehensive and accurate multimodal response generation.

The MMGraphRAG framework offers several notable advantages. First, by modeling images as independent nodes, the framework enhances cross-modal reasoning capabilities. This design provides strong support for sophisticated cross-modal inference tasks. Finally, by constructing the MMKG based on LLMs, the framework eliminates reliance on training, offering enhanced flexibility.

3.2 Image2Graph

To realize MMGraphRAG, fine-grained entity-level processing of visual data is crucial. Constructing accurate and comprehensive scene graphs plays a key role, but traditional methods often overlook fine-grained semantic details and fail to account for hidden information between objects, leading to inadequate scene graphs and reasoning bias in downstream tasks [36, 37].

In contrast, MLLM-based methods can extract entities and infer implicit relations through semantic segmentation and reasoning ability of MLLM, generating both high-precision and fine-grained scene graphs [7, 58]. These methods capture both explicit spatial relations (e.g., *girl—girl holding a camera—camera*) and implicit ones (e.g., *boy—the boy and girl appear to be close, possibly friends or a couple—girl*). Furthermore, they provide richer semantic descriptions for visual entities, refining basic labels such as *boy* into more detailed expressions like *a college student with tired eyes*. Unlike methods relying on large-scale annotated datasets [33, 50, 51, 63, 68, 71], MLLM-based methods improve generalization capabilities by minimizing human supervision.

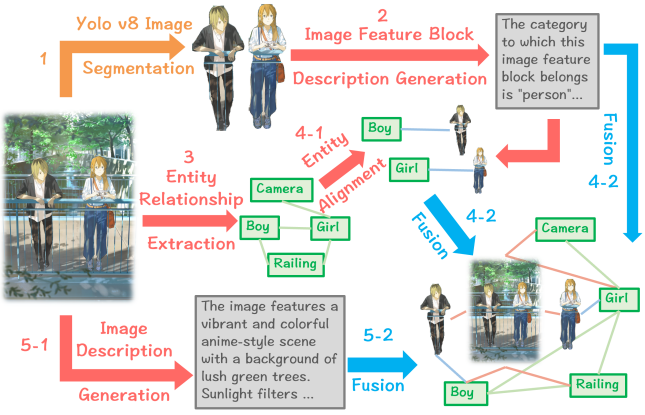

Figure 3: An Example of the Img2Graph Module in Action

The Img2Graph module maps images into KGs through a five-step pipeline. First, semantic segmentation is performed using YOLO [55] to divide the image into semantically independent regions, referred to as image feature blocks. Second, MLLMs generate textual descriptions for each feature block. Third, entities and their relations are extracted from the image. Fourth, MLLMs align the segmented feature blocks with the extracted entities. Fifth, a global entity is constructed to describe the entire image and to establish connections with local entities. A detailed example is illustrated in Figure 3.

Through this pipeline, Img2Graph produces scene graphs with explicit structure and enriched semantics, transforming raw visual inputs into KGs. Each feature block possesses clear physical boundaries and, with the aid of MLLMs, is assigned accurate and informative descriptions. The resulting multimodal scene graphs not only enhance the structural representation of visual content but also strengthen contextual relevance in multimodal semantic retrieval. This extends GraphRAG with improved retrievability and clearer reasoning paths, substantially enhancing the robustness and accuracy of the RAG process in complex query scenarios.

3.3 Cross-modal Fusion Module

The core objective of cross-modal fusion is to construct a unified MMKG by aligning and fusing entities from both image-based and text-based KGs. This process not only ensures deep semantic alignment between modalities, but also significantly enhances the logical coherence and informational completeness of the resulting MMKG. Specifically, our cross-modal fusion framework consists of the following key components:

3.3.1 Fine-Grained Entity Alignment Between KGs. The first and most crucial step of cross-modal fusion is aligning entities extracted from image and text modalities, which is essentially Cross-Modal Entity Linking (CMEL).

CMEL Task Definition. Define image set as $I = \{I_1, I_2, \ldots, I_N\}$, where each image I_i contains a set of extracted entities denoted by: $E(I_i) = \{e_1^{(I_i)}, e_2^{(I_i)}, \ldots, e_K^{(I_i)}\}$.

Similarly, define the text set as $T = \{T_1, T_2, \ldots, T_M\}$, where each text chunk T_j contains a set of extracted entities: $E(T_j) = \{e_1^{(T_j)}, e_2^{(T_j)}, \ldots, e_L^{(T_j)}\}$.

The goal of CMEL is to identify pairs of entities from images and text that refer to the same real-world concept. In other words, for each visual entity $e_k^{(I_i)}$, we aim to align it with the most semantically relevant textual entity $e_l^{(T_j)}$. Since the number of textual entities is generally larger than that of visual entities, the task is decomposed into two stages: (1) generating a set of candidate textual entities for each visual entity, and (2) selecting the best-aligned textual entity from this set.

Formally, for each visual entity $e_k^{(I_i)}$, define the candidate set as:

$$C(e_k^{(I_i)}) \subseteq \bigcup_{j-1}^{j+1} E(T_j),$$

where $C(e_k^{(I_i)})$ contains the most relevant textual entities selected from the textual entity pool of the context.

The final alignment is determined by maximizing a similarity function f, such that:

$$\mathcal{A}(e_k^{(I_i)}) = \arg \max_{e \in C(e_k^{(I_i)})} f(e_k^{(I_i)}, e).$$

Once aligned, the linked entity pairs are passed to an LLM-based module to ensure they share a unified representation in the KG.

SpecLink:A Spectral Clustering–Based Candidate Generation. To improve the efficiency and robustness of candidate entities generation, we propose SpecLink, a spectral clustering-based optimization strategy. Existing methods fall into two categories: (1) *distance-based clustering*, such as KMeans [25, 31, 48] and DBSCAN [13, 24], which depends semantic similarity but ignores graph structure, and (2) *graph-based clustering*, such as PageRank [1] and Leiden [53], which captures structural relations but suffers in sparse graphs. To address both aspects, we design SpecLink tailored for CMEL.

Specifically, we redesign the weighted adjacency matrix $\mathbf{A}$ and the degree matrix $\mathbf{D}$ to capture both semantic and structural information between entities.

The adjacency matrix $\mathbf{A}$ is constructed to reflect the similarity between nodes as well as the importance of their relations. It is defined as:

$$\mathbf{A}_{pq} = sim(\mathbf{v}_p, \mathbf{v}_q) \cdot weight(r_{pq}) \tag{1}$$

where $\mathbf{v}_p$ is the embedding vector of entity e_p, and $sim(\cdot)$ denotes cosine similarity. The term r_{pq} represents the relation between e_p and e_q in the KG, and $weight(r_{pq})$ is a scalar reflecting the importance of the relation assessed by LLMs. If no relation exists between two entities, we set $weight(r_{pq}) = 1$.

The degree matrix $\mathbf{D}$ is a diagonal matrix, where each diagonal entry $\mathbf{D}_{pp}$ indicates the connectivity strength of node p, computed as:

$$\mathbf{D}_{pp} = \sum_q \mathbf{A}_{pq}.$$

Intuitively, each diagonal value in D represents the total weighted similarity between node p and all other nodes.

Following the standard spectral clustering procedure, we construct the Laplacian matrix and perform eigen-decomposition. We then form the matrix $\mathbf{Q} = [\mathbf{u}_1, \ldots, \mathbf{u}_m]$ using the smallest m eigenvectors, where m depends on the number of textual entities in context [22].

Clustering is performed on the row space of $\mathbf{Q}$ using DBSCAN to obtain cluster partitions:

$$\text{Cluster}(\mathbf{Q}) = \{C_1, C_2, \ldots, C_n\}.$$

For each image entity $e_k^{(I_i)}$, we select the most relevant cluster based on the cosine similarity between its embedding $\mathbf{v}_k^{(I_i)}$ and the cluster members. The candidate entity set is then defined as:

$$C(e_k^{(I_i)}) = \bigcup_{C_n} \{e_p \mid e_p \in C_n\}.$$

Finally, we perform entity alignment using LLM-based inference, which has demonstrated high accuracy and adaptability in complex alignment scenarios [38, 39]. The prompt includes:

- the name and description of the visual entity,
- descriptions of candidate entities from the selected cluster, and
- a fixed set of alignment examples.

The output is adopted as the final alignment result.

3.3.2 Enhancing Remaining Image Entities. Then, we enhance the descriptions of remaining visual entities not aligned during CMEL by incorporating semantically relevant information from the original text to improve the completeness of the image-based KG.

For instance, while the original text may only state that *"HURRICANE SLAMS COASTAL REGIONS IN WEST FLORIDA..."*, the corresponding image depicts *a flooded neighborhood* without explicit textual alignment. By integrating contextual cues such as *Hurricane Ian* and *Florida* from the text, the visual entity can be enriched into *"A neighborhood in Florida severely flooded by Hurricane Ian, causing significant damage and displacement."* This step ensures high-fidelity entity descriptions and enhances the internal completeness of the MMKG.

3.3.3 Aligning Global Image Entity with Relevant Textual Entity. In addition to fine-grained alignment, we align the global entity of each image with relevant textual entity. If no direct match is found, we create a new entity in the text-based KG to represent the overall semantic content of the image. This step ensures that holistic semantic information is preserved and cross-modal coherence is maintained.

3.3.4 Entity Fusion for Unified Representation. For all aligned entities, we perform semantic fusion to ensure unified representations in the MMKG. This step guarantees consistent alignment and representation of entities across modalities, facilitating downstream reasoning and retrieval.

3.3.5 Iterative Graph Construction. The above steps are repeated for each image to construct a thorough MMKG.

4 Experiments

In this section, we present a comprehensive empirical evaluation of the proposed MMGraphRAG framework. Our evaluation is structured in three main parts. First, we conduct a targeted experiment on the CMEL task to specifically validate the effectiveness of our SpecLink method for generating candidate entities. Second, we assess the end-to-end performance of the complete MMGraphRAG system on two challenging multimodal Document Question Answering (DocQA) benchmarks, DocBench and MMLongBench, comparing it against a suite of baseline methods. Finally, to provide deeper insight into our model's architecture, we conclude with a series of ablation studies that analyze the crucial roles of the cross-modal fusion module and the explicit graph-based representation.

4.1 CMEL Experiments

To evaluate the effectiveness of our SpecLink method for the CMEL task, we construct a novel CMEL benchmark. Designed for fine-grained multi-entity alignment in complex multimodal scenarios, the CMEL dataset exhibits significantly greater entity diversity and relation complexity compared to existing benchmarks such as MATE[5]. Moreover, CMEL dataset is released as an open-source benchmark and supports extensibility through a semi-automated

construction pipeline. This pipeline enables users to incorporate minimal human supervision to generate new samples, providing a sustainable experimental foundation for future research in the CMEL task. Please refer to the anonymized supplementary materials (linked in the Appendix) for additional details on the construction process, dataset description, illustrative examples, and reliability validation.

4.1.1 CMEL Dataset. The CMEL dataset comprises documents from three distinct domains—news, academia, and novels—ensuring broad domain diversity and practical applicability, illustrated in Figure 4. Each sample includes (i) a text-based KG built from text chunks, (ii) an image-based KG derived from per-image scene graphs, and (iii) the original PDF-format document. In total, CMEL provides 1,114 alignment instances-87 drawn from news articles, 475 from academic papers, and 552 from novels. Gold alignments are constructed through a semi-automatic entity fusion pipeline followed by manual verification. A random manual inspection of 20% of the data reports 97.7% coverage of entities requiring fusion and 99.0% correctness of the merged entities, indicating that the evaluation labels are highly reliable.

To comprehensively assess performance, we adopt both micro-accuracy and macro-accuracy as evaluation metrics. Micro-accuracy is computed on a per-entity basis, reflecting the overall prediction correctness and serving as an indicator of global performance. Meanwhile, macro-accuracy calculates the average accuracy per document, mitigating evaluation bias caused by imbalanced entity distributions across documents and better highlighting performance of different methods across diverse domains.

4.1.2 Experimental Setup and Results. We conduct a series of comparative experiments based on the CMEL dataset. The experiments cover three categories of unsupervised approaches: embedding-based methods (Emb), LLM-based methods (LLM), and our proposed SpecLink method (Spec). We further compare against multiple mainstream clustering algorithms to provide comprehensive baselines.

The embedding-based method encodes visual and textual entities into vector representations using a pretrained embedding model, and then computes their semantic proximity via cosine similarity. A textual entity is considered a candidate if the similarity score exceeds a predefined threshold.

The LLM-based method leverages the reasoning capabilities of LLMs to directly generate candidate sets. Specifically, the model is prompted with an visual entity, its surrounding context, and a pool of textual entities. It then outputs the most plausible candidate entities based on contextual understanding.

For clustering-based baselines, we include DBSCAN (DB), KMeans (KM), PageRank (PR), and Leiden (Lei).

Entity alignment within candidate sets is uniformly conducted via LLM-based reasoning.

To ensure the robustness and generalizability of our results, evaluations are conducted on different models. Due to space limitations, we report only the best-performing configurations for each method category in the results table. Specifically, the experiments utilize the embedding model stella-en-1.5B-v5 [4], the LLM Qwen2.5-72B-Instruct [52], and the MLLM InternVL2.5-38B-MPO [60]. All results are averaged over three runs with different random seeds. Across runs, the standard deviation of micro and macro accuracy is below 0.5 percentage points on all domains and methods.

Meth.	micro/macro Acc.			Overall.
	News	Aca.	Nov.	
Emb	10.8/8.4	33.1/34.5	9.0/7.5	20.0/16.8
LLM	33.3/24.1	36.8/36.1	17.4/20.8	27.1/27.0
DB	53.8/45.9	60.8/58.3	29.9/34.2	45.2/46.1
KM	50.5/40.6	60.7/57.7	29.6/30.5	45.2/43.0
PR	51.6/44.4	59.7/56.8	29.1/35.2	44.1/45.5
Lei	54.8/44.7	60.5/55.5	29.4/30.6	44.8/43.6
Spec	**65.5/56.9**	**73.3/69.9**	**31.2/39.4**	**51.8/59.2**

Table 1: Micro/macro accuracy (%) on CMEL dataset. Results are averaged over three random seeds.

The results are shown in Table 1. We further perform a paired bootstrap test over entity-level predictions between SpecLink and the strongest baseline (DBSCAN). The improvements in overall micro and macro accuracy are statistically significant with $p < 0.01$ on the CMEL dataset. Overall, clustering-based methods significantly outperform the embedding-based and LLM-based methods in the CMEL task. Compared to other clustering-based methods, SpecLink achieves the best performance, improving micro-accuracy by about 15% and macro-accuracy by around 30%, clearly demonstrating its effectiveness in CMEL task.

4.2 Multimodal Document QA Experiments

We choose DocQA as the primary evaluation task for MMGraphRAG because it comprehensively assesses the capabilities of method in multimodal information integration, complex reasoning, and domain adaptability. DocQA task involves deep understanding of long documents and the integration of diverse formats. Furthermore, documents from different domains exhibit unique terminologies and structural patterns, requiring methods to adapt flexibly. These characteristics make multimodal DocQA a challenging and comprehensive benchmark for evaluating the performance of MMGraphRAG.

4.2.1 Benchmarks. DocBench contains 229 PDF documents from publicly available online resources, covering five domains: academia (Aca.), finance (Fin.), government (Gov.), laws (Law.), and news (News). It includes four types of questions: pure text questions (Txt.), multimodal questions (Mm.), metadata questions, and unanswerable questions (Una.). For our experiments, since the information is converted into KGs, we do not focus on metadata. Therefore, this category of questions is excluded from statistics. We strictly follow the official evaluation protocol of DocBench, which relies on an LLM judge to determine the correctness of model answers. The judge is provided with the question, the reference answer, the model prediction, and the supporting evidence extracted from the original document, and then returns a binary decision on whether the prediction is correct.

MMLongBench consists of 135 long PDF documents collected from seven different domains. It evaluates multimodal reasoning

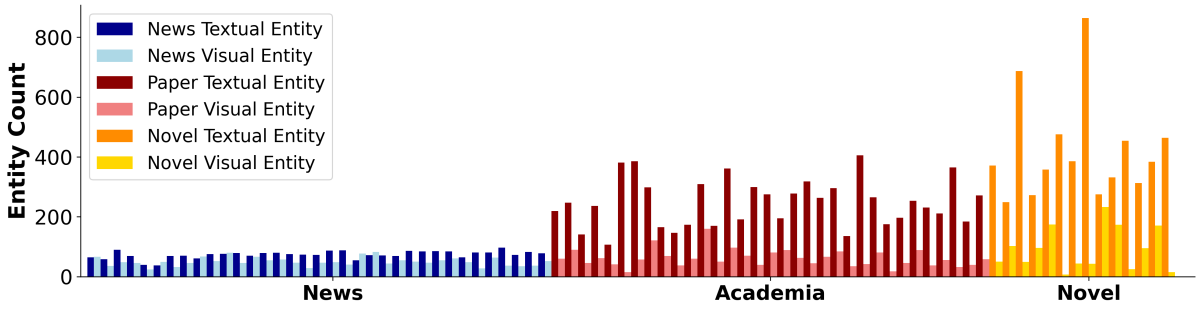

Figure 4: Entity Distribution Across Document Domains. The figure illustrates how entity types and quantities vary among news, academic papers, and novels, demonstrating the dataset's diversity and the challenge of cross-modal entity alignment.

across various content types. The Locations dimension indicates whether the supporting evidence for an answer is contained within a single page (Sin.) or spans multiple pages (Mul.) of a document, while Formats represent different content sources. MMLongBench further includes annotations covering multiple modalities—such as text (Txt.), charts (Cha.), tables (Tab.), layout (Lay.), and figures (Fig.)—to comprehensively assess document understanding. Following the original benchmark, we adopt the three-step evaluation protocol of MATHVISTA [40]: response generation, answer extraction using an LLM, and score calculation via an LLM judge.

In all DocBench and MMLongBench experiments, the judge model is fixed to Llama3.1-70B-Instruct. The judge is invoked with temperature 0 and greedy decoding, and the judging prompts are kept identical for all compared methods. Accuracy is reported as the sole evaluation metric to measure the correctness of model predictions.

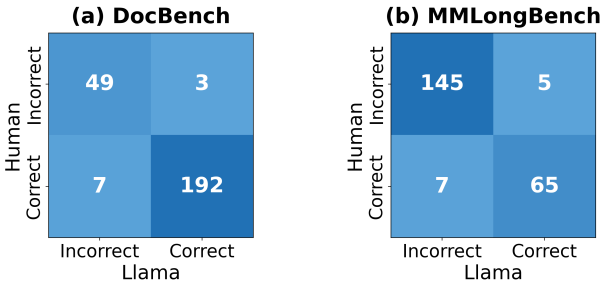

Figure 5: Confusion matrices comparing human majority votes with Llama3.1-70B-Instruct as an automatic judge on (a) DocBench and (b) MMLongBench. The LLM judge exhibits strong alignment with human judgments across both datasets.

4.2.2 Reliability of LLM-as-a-Judge Evaluation. Although using large language models as automatic judges has become standard practice in recent multimodal QA research [11, 15, 29, 42, 44, 73], it may still introduce biases. To assess the reliability of our evaluation protocol, we conduct a human-LLM consistency study.

We randomly sample 50 documents from DocBench and 25 from MMLongBench along with all associated questions, and collect human judgments (correct vs. incorrect) for all answers produced by our best-performing configuration. Human labels are aggregated through majority voting.

Agreement with Human Judgments. Figure 5 shows the confusion matrices comparing the decisions of the LLM judge (Llama3.1-70B-Instruct) with human majority votes on DocBench (Figure 5a) and MMLongBench (Figure 5b). On the DocBench portion of the subset, Llama achieves an agreement of **96.0%** with human majority labels and a Cohen's κ of **0.882**. On the MMLongBench portion, the agreement remains similarly high at **94.6%**, with a κ of **0.876**. These values fall in the "almost perfect" agreement range, indicating that the automatic scores are highly consistent with human evaluations.

These results demonstrate that the automatic evaluation scores used in this work are highly consistent with human assessment. While LLM-based evaluation may still introduce subtle biases—a limitation shared by most recent multimodal DocQA benchmarks—the strong consistency observed here suggests that its impact on our comparative results is minimal.

4.2.3 Comparison with Basic Methods. To ensure fair comparisons, eliminate potential biases arising from using the same model for both generation and evaluation, and assess the general applicability of our proposed prompt, this experiment selects various LLMs and MLLMs as comparison benchmarks. Although our experiments initially evaluated a broader set of three LLMs, namely Llama3.1-70B-Instruct [2], Qwen2.5-72B-Instruct [64], and Mistral-Large-Instruct-2411 [3], and three MLLMs, including Ovis1.6-Gemma2-27B [41], Qwen2-VL-72B [59], and InternVL2.5-38B-MPO [10], we focus our analysis on four representative models for clarity. Specifically, we present a comparison between Llama3.1(L) and Qwen2.5(Q) for LLMs, and between Qwen2(Qv) and InternVL2.5(Iv) for MLLMs.

We consider the following baselines:

LLM: We replace images with MLLM generated corresponding text after reprocessing. All text and questions are input into the LLM. If the content exceeds the model's context length, it will be divided into parts, and partial answers are concatenated as final results.

Method	Domains					Modalities			Overall Acc.
	Aca.	Fin.	Gov.	Laws	News	Text.	Multi.	Una.	
LLM(L)	43.9	13.5	53.4	44.5	79.7	52.9	18.8	**81.5**	44.7
LLM(Q)	41.3	16.3	50.7	49.7	77.3	53.9	20.1	75.8	44.8
MLLM(Qv)	17.5	14.9	25.0	34.6	48.8	34.0	8.4	40.3	25.4
MLLM(Iv)	19.8	16.3	28.4	31.4	46.5	35.7	15.9	39.5	27.7
NR(L)	43.6	38.2	66.2	64.9	**80.2**	79.9	32.1	70.2	61.0
NR(Q)	43.6	34.4	62.8	65.4	75.0	81.6	30.5	67.7	59.5
GR(L)	40.6	27.1	56.8	59.7	75.0	73.5	24.4	76.6	54.7
GR(Q)	39.6	25.7	52.5	49.7	74.5	71.7	26.0	67.5	52.3
MGR(L-Qv)	51.8	59.4	62.8	60.7	77.9	79.1	77.8	70.2	74.0
MGR(Q-Qv)	51.8	62.9	**66.9**	68.6	76.2	**82.4**	81.1	67.7	75.2
MGR(L-Iv)	**60.7**	64.1	62.6	64.9	76.2	80.0	86.4	75.0	**77.5**
MGR(Q-Iv)	60.5	**65.8**	66.5	**70.4**	77.1	81.2	**88.7**	71.9	76.8

Table 2: Accuracy of different methods on DocBench across domains and modalities

Method	Formats					Locations			Overall Acc.
	Cha.	Tab.	Txt.	Lay.	Fig.	Sin.	Mul.	Una.	
LLM(L)	16.3	12.7	32.1	21.9	17.4	23.7	20.3	51.6	28.2
LLM(Q)	16.8	12.6	33.3	23.5	16.1	22.5	20.0	53.2	27.8
MLLM(Qv)	7.6	5.4	10.0	8.8	12.7	10.8	9.9	8.1	10.0
MLLM(Iv)	8.8	8.1	10.7	11.8	11.4	13.3	7.9	13.9	11.6
NR(L)	16.3	15.3	31.0	22.7	18.7	24.9	19.5	56.5	29.2
NR(Q)	15.1	10.8	30.3	20.3	14.9	22.3	16.4	52.5	26.2
GR(L)	7.6	6.7	25.1	15.0	10.6	16.3	12.3	**78.5**	27.2
GR(Q)	14.0	11.0	26.1	12.2	8.5	18.2	13.2	77.1	28.1
MGR(L-Qv)	26.4	29.2	26.4	13.8	21.2	37.6	13.8	55.2	32.6
MGR(Q-Qv)	26.2	30.0	29.3	**29.1**	29.2	38.7	20.1	51.6	34.8
MGR(L-Iv)	34.7	**36.6**	31.9	12.9	28.5	38.7	21.9	59.2	36.9
MGR(Q-Iv)	**34.7**	36.5	**33.8**	28.7	**34.6**	**39.6**	**26.7**	55.8	**38.8**

Table 3: Accuracy of different methods on MMLongBench across formats and locations

MLLM: All images are concatenated and resized based on model constraints. These image blocks, along with the question, are input into the MLLM to test its ability to reason over multimodal data.

NaiveRAG [27] (NR): The text is chunked into segments of 500 tokens. Each chunk and question is embedded. Then, the top-k relevant chunks (10 selected) are retrieved by calculating cosine similarity with the question, and these relevant chunks are provided along with the question to LLMs.

GraphRAG (GR): The GraphRAG method was modified by removing the community detection part and using local mode querying to ensure fair comparison with other methods [14, 19]. The top-k entities (10 selected) are used for retrieval, with the length of the text of entities and relations limited to a maximum of 4000 tokens, and the maximum number of chunks is 10.

We compared multiple methods and highlighted the advantages of MMGraphRAG (MGR) over other methods.

The results for the DocBench and MMLongBench datasets are presented in Table 2 and Table 3, respectively. The following analysis from several key perspectives explains the superiority of MMGraphRAG.

Domain Adaptability. Compared to all text-only RAG methods, MMGraphRAG shows substantial gains in domains with high visual-structural complexity, such as academia and finance(MGR 60.7% vs. NR 43.6%; MGR 65.8% vs. NR 38.2% on DocBench). This indicates that MMGraphRAG performs well in specialized fields while retaining the ability to generalize across diverse domains. Its flexibility and adaptability make it well-suited for real-world applications involving heterogeneous multimodal documents.

Multimodal Information Processing Capability. Counterintuitively, results show that MLLMs alone do not outperform other methods on vision-centric queries, even worse than NaiveRAG based on image captioning. MMGraphRAG achieves a substantial improvement in multimodal query accuracy on DocBench (88.7%), far surpassing both the NaiveRAG (32.1%) and GraphRAG (26.0%), demonstrating its superior ability to retrieve and utilize visual knowledge. Similarly, on MMLongBench, MMGraphRAG attains the highest performance in charts, tables, figures and layout reasoning (34.7%, 36.6%, 29.1% and 34.6%), which are the most visually demanding tasks, confirming its effectiveness in fusing structural and semantic cues from complex multimodal inputs. These results validate that MMGraphRAG's explicit MMKG construction provides enhanced accuracy, setting a new standard for multimodal information processing.

4.3 Ablation Study

To investigate the individual contributions of our key components, we conduct a series of ablation studies. We aim to answer two primary questions: 1) How crucial is our sophisticated cross-modal fusion module? 2) What are the benefits of constructing an explicit MMKG compared to Multimodal RAG (MRAG) approaches?

4.3.1 Impact of the Cross-Modal Fusion Module. The ablation results highlight how removing the fusion module significantly degrades multimodal reasoning. To validate the necessity of our fusion module, we design a simplified baseline, MMGraphRAG (w/o Fusion). In this variant, the cross-modal fusion module is replaced with a naive method that performs entity alignment based solely on embedding similarity. An image entity and a text entity are considered aligned if the cosine similarity of their embeddings exceeds a predefined threshold (0.7 in our experiments). The threshold is selected on a held-out development split of the academia subset by grid-searching over $\{0.6, 0.65, 0.7, 0.75\}$ to maximize micro-accuracy. All other components, including the backbone LLM/MLLM configuration, retrieval settings, and the LLM-as-a-judge evaluation protocol, are kept identical to the full MMGraphRAG model to ensure a controlled comparison.

We conduct this experiment on the academia (Aca) subset of DocBench, chosen for its high density of multimodal questions, making it an ideal testbed for evaluating fusion performance. The results are presented in Figure 6.

The analysis of the results reveals several key insights:

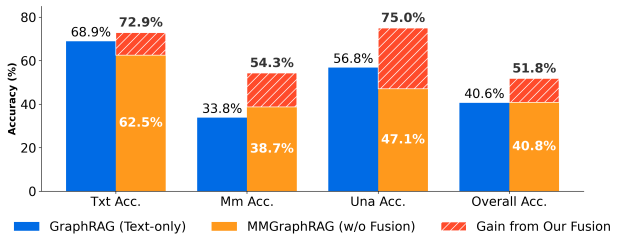

Figure 6: Impact of Cross-Modal Fusion Module by Metric

- **Textual Performance:** Interestingly, the naive fusion approach degrades performance on text-only (Txt) questions. This suggests that imprecise entity linking introduces noise and irrelevant visual context, which can disrupt purely textual reasoning. In contrast, our full model enhances text accuracy, indicating that well-aligned visual information can effectively supplement textual context, clarifying ambiguities and providing missing details.
- **Multimodal Performance:** On multimodal (Mm) questions, simply incorporating the image KG with a naive alignment yields a marginal improvement (+4.9%) over the text-only GraphRAG. However, our full MMGraphRAG framework achieves a substantial gain (+21.5%). This demonstrates that the fusion method is essential for building precise and meaningful cross-modal links, which are critical for answering complex multimodal queries.
- **Hallucination Suppression:** The most significant difference is observed in unanswerable (Una) questions. The naive fusion method's accuracy drops sharply (-9.7%), showing that introducing poorly aligned visual information acts as noise and exacerbates model hallucinations. Conversely, our method's robust fusion process strengthens the logical coherence between modalities, improving the model's ability to identify unanswerable questions by a remarkable 18.2%. This confirms that our fusion method builds authentic and valuable connections rather than spurious correlations.

These results collectively underscore that our proposed cross-modal fusion module is a critical component, not just an incremental improvement.

4.3.2 Comparison with MRAG Methods. To isolate the benefits of our structured MMKG, we compare MMGraphRAG against a representative MRAG framework, M3DOCRAG (M3DR). This comparison effectively serves as an ablation of our explicit graph-building pipeline, contrasting it with approaches that typically project multimodal features into a shared embedding space for retrieval. For a fair comparison, both methods use the Qwen2.5-7B-Instruct model as the LLM and the Qwen2-VL-7B model as the MLLM, and share the same retrieval configuration (chunk size, top-k) and prompting strategy. The experiment is conducted on the MMLongBench dataset, and the results are shown in Table 4.

The results highlight the advantages of our MMKG-based approach. By explicitly modeling relationships between visual and textual entities, MMGraphRAG more effectively handles queries requiring deep semantic alignment between images and text. This

Method	Formats					Locations			Overall Acc.
	Cha.	Tab.	Txt.	Lay.	Fig.	Sin.	Mul.	Una.	
M3DR	18.9	20.1	30.0	23.5	20.8	32.4	14.8	5.8	21.0
MGR	**21.1**	**27.1**	24.6	18.2	22.2	34.3	12.5	**35.1**	**26.5**

Table 4: Performance comparison between M3DOCRAG and MMGraphRAG

is particularly evident in its superior performance on questions related to charts and tables (Cha. and Tab.), where it outperforms M3DR by a significant margin (48.2% vs. 39.0%).

Furthermore, ablating our explicit graph structure in favor of an MRAG approach reveals a critical weakness in handling unanswerable (Una) questions. MRAG methods, which rely on a unified embedding space, can be misled by noisy but semantically adjacent evidence, causing the model to confidently generate incorrect answers. In contrast, the structured reasoning enabled by our MMKG allows the model to more reliably traverse evidence and assess its completeness. This structured approach significantly reduces the generation of misleading answers and enhances the model's robustness, as shown by the massive performance gap on unanswerable questions (MMGR 35.1% vs. M3DR 5.8%).

This analysis validates that the explicit construction of an MMKG is a crucial design choice for achieving robust and accurate multimodal DocQA, particularly in complex scenarios requiring nuanced, cross-modal reasoning.

5 Conclusion

We propose MMGraphRAG, a framework that integrates textual and image data into a multimodal knowledge graph to facilitate deep cross-modal fusion and reasoning. Experimental results demonstrate that MMGraphRAG outperforms all kinds of existing RAG methods on multimodal DocQA tasks. The framework exhibits strong domain adaptability and produces traceable reasoning paths. We hope this work will inspire further research on cross-modal entity linking and the development of graph-based frameworks for deeper and more comprehensive multimodal reasoning.

References

[1] Shayan A. Tabrizi, Azadeh Shakery, Masoud Asadpour, Maziar Abbasi, and Mohammad Ali Tavallaie. 2013. Personalized PageRank Clustering: A graph clustering algorithm based on random walks. *Physica A: Statistical Mechanics and its Applications* 392, 22 (2013), 5772–5785. doi:10.1016/j.physa.2013.07.021
[2] Meta AI. 2024. LLaMA-3.1-70B-Instruct. Available at https://huggingface.co/meta-llama/Llama-3.1-70B-Instruct.
[3] Mistral AI. 2024. Mistral-Large-Instruct-2411. Available at https://huggingface.co/mistralai/Mistral-Large-Instruct-2411.
[4] Stability AI. 2024. stella-en-1.5B-v5. https://huggingface.co/stabilityai/stella-en-1.5B-v5. Open-weight English language model.
[5] Iñigo Alonso, Gorka Azkune, Ander Salaberria, Jeremy Barnes, and Oier Lopez de Lacalle. 2025. Vision-Language Models Struggle to Align Entities across Modalities. arXiv:2503.03854 [cs.CL] https://arxiv.org/abs/2503.03854
[6] Chenyang Bu, Guojie Chang, Zihao Chen, Cunyuan Dang, Zhize Wu, Yi He, and Xindong Wu. 2025. Query-Driven Multimodal GraphRAG: Dynamic Local Knowledge Graph Construction for Online Reasoning. In *Findings of the Association for Computational Linguistics: ACL 2025*. 21360–21380.
[7] Guikun Chen, Jin Li, and Wenguan Wang. 2024. Scene Graph Generation with Role-Playing Large Language Models. In *Advances in Neural Information Processing Systems*, A. Globerson, L. Mackey, D. Belgrave, A. Fan, U. Paquet, J. Tomczak, and C. Zhang (Eds.), Vol. 37. Curran Associates, Inc.,

132238–132266. https://proceedings.neurips.cc/paper_files/paper/2024/file/ee74a6ade401e200985e2421b20bbae4-Paper-Conference.pdf

[8] Jianlv Chen, Shitao Xiao, Peitian Zhang, Kun Luo, Defu Lian, and Zheng Liu. 2024. Bge m3-embedding: Multi-lingual, multi-functionality, multi-granularity text embeddings through self-knowledge distillation. *arXiv preprint arXiv:2402.03216* (2024).

[9] Yixiang Chen, Penglei Sun, Xiang Li, and Xiaowen Chu. 2025. MRD-RAG: Enhancing Medical Diagnosis with Multi-Round Retrieval-Augmented Generation. arXiv:2504.07724 [cs.CL] https://arxiv.org/abs/2504.07724

[10] Zhe Chen, Jiannan Wu, Wenhai Wang, Weijie Su, Guo Chen, Sen Xing, Muyan Zhong, Qinglong Zhang, Xizhou Zhu, Lewei Lu, et al. 2024. Internvl: Scaling up vision foundation models and aligning for generic visual-linguistic tasks. In *Proceedings of the IEEE/CVF conference on computer vision and pattern recognition*. 24185–24198.

[11] Jaemin Cho, Debanjan Mahata, Ozan Irsoy, Yujie He, and Mohit Bansal. 2024. M3DocRAG: Multi-modal Retrieval is What You Need for Multi-page Multi-document Understanding. *CoRR* abs/2411.04952 (2024). https://doi.org/10.48550/arXiv.2411.04952

[12] Yun-Wei Chu, Kai Zhang, Christopher Malon, and Martin Renqiang Min. 2025. Reducing Hallucinations of Medical Multimodal Large Language Models with Visual Retrieval-Augmented Generation. In *Workshop on Large Language Models and Generative AI for Health at AAAI 2025*. https://openreview.net/forum?id=A4RH0kNxpn

[13] Dingsheng Deng. 2020. DBSCAN Clustering Algorithm Based on Density. In *2020 7th International Forum on Electrical Engineering and Automation (IFEEA)*. 949–953. doi:10.1109/IFEEA51475.2020.00199

[14] Darren Edge, Ha Trinh, Newman Cheng, Joshua Bradley, Alex Chao, Apurva Mody, Steven Truitt, and Jonathan Larson. 2024. From local to global: A graph rag approach to query-focused summarization. *arXiv preprint arXiv:2404.16130* (2024).

[15] Darren Edge, Ha Trinh, Newman Cheng, Joshua Bradley, Alex Chao, Apurva Mody, Steven Truitt, Dasha Metropolitansky, Robert Osazuwa Ness, and Jonathan Larson. 2025. From Local to Global: A Graph RAG Approach to Query-Focused Summarization. arXiv:2404.16130 [cs.CL] https://arxiv.org/abs/2404.16130

[16] Manuel Faysse, Hugues Sibille, Tony Wu, Bilel Omrani, Gautier Viaud, CELINE HUDELOT, and Pierre Colombo. 2025. ColPali: Efficient Document Retrieval with Vision Language Models. In *The Thirteenth International Conference on Learning Representations*. https://openreview.net/forum?id=ogjBpZ8uSi

[17] Jingru Gan, Jinchang Luo, Haiwei Wang, Shuhui Wang, Wei He, and Qingming Huang. 2021. Multimodal Entity Linking: A New Dataset and A Baseline. In *Proceedings of the 29th ACM International Conference on Multimedia* (Virtual Event, China) *(MM '21)*. Association for Computing Machinery, New York, NY, USA, 993–1001. doi:10.1145/3474085.3475400

[18] Gongde Guo, Hui Wang, David Bell, Yaxin Bi, and Kieran Greer. 2003. KNN model-based approach in classification. In *On The Move to Meaningful Internet Systems 2003: CoopIS, DOA, and ODBASE: OTM Confederated International Conferences, CoopIS, DOA, and ODBASE 2003, Catania, Sicily, Italy, November 3-7, 2003. Proceedings*. Springer, 986–996.

[19] Zirui Guo, Lianghao Xia, Yanhua Yu, Tu Ao, and Chao Huang. 2024. Lightrag: Simple and fast retrieval-augmented generation. *arXiv preprint arXiv:2410.05779* (2024).

[20] Mahd Hindi, Linda Mohammed, Ommama Maaz, and Abdulmalik Alwarafy. 2025. Enhancing the Precision and Interpretability of Retrieval-Augmented Generation (RAG) in Legal Technology: A Survey. *IEEE Access* 13 (2025), 46171–46189. doi:10.1109/ACCESS.2025.3550145

[21] Lei Huang, Weijiang Yu, Weitao Ma, Weihong Zhong, Zhangyin Feng, Haotian Wang, Qianglong Chen, Weihua Peng, Xiaocheng Feng, Bing Qin, and Ting Liu. 2025. A Survey on Hallucination in Large Language Models: Principles, Taxonomy, Challenges, and Open Questions. *ACM Trans. Inf. Syst.* 43, 2, Article 42 (Jan. 2025), 55 pages. doi:10.1145/3703155

[22] Hongjie Jia, Shifei Ding, Xinzheng Xu, and Ru Nie. 2014. The latest research progress on spectral clustering. *Neural Computing and Applications* 24 (2014), 1477–1486.

[23] Glenn Jocher, Ayush Chaurasia, and Jing Qiu. 2023. Ultralytics YOLO v8. Available at https://github.com/ultralytics/ultralytics.

[24] Kamran Khan, Saif Ur Rehman, Kamran Aziz, Simon Fong, and S. Sarasvady. 2014. DBSCAN: Past, present and future. In *The Fifth International Conference on the Applications of Digital Information and Web Technologies (ICADIWT 2014)*. 232–238. doi:10.1109/ICADIWT.2014.6814687

[25] Trupti M Kodinariya, Prashant R Makwana, et al. 2013. Review on determining number of Cluster in K-Means Clustering. *International Journal* 1, 6 (2013), 90–95.

[26] Woosuk Kwon, Zhuohan Li, Siyuan Zhuang, Ying Sheng, Lianmin Zheng, Cody Hao Yu, Joseph Gonzalez, Hao Zhang, and Ion Stoica. 2023. Efficient memory management for large language model serving with pagedattention. In *Proceedings of the 29th Symposium on Operating Systems Principles*. 611–626.

[27] Patrick Lewis, Ethan Perez, Aleksandra Piktus, Fabio Petroni, Vladimir Karpukhin, Naman Goyal, Heinrich Küttler, Mike Lewis, Wen-tau Yih, Tim Rocktäschel, et al. 2020. Retrieval-augmented generation for knowledge-intensive nlp tasks. *Advances in neural information processing systems* 33 (2020), 9459–9474.

[28] Patrick Lewis, Ethan Perez, Aleksandra Piktus, Fabio Petroni, Vladimir Karpukhin, Naman Goyal, Heinrich Küttler, Mike Lewis, Wen-tau Yih, Tim Rocktäschel, Sebastian Riedel, and Douwe Kiela. 2020. Retrieval-Augmented Generation for Knowledge-Intensive NLP Tasks. In *Advances in Neural Information Processing Systems*, H. Larochelle, M. Ranzato, R. Hadsell, M.F. Balcan, and H. Lin (Eds.), Vol. 33. Curran Associates, Inc., 9459–9474. https://proceedings.neurips.cc/paper_files/paper/2020/file/6b493230205f780e1bc26945df7481e5-Paper.pdf

[29] Zhuoqun Li, Xuanang Chen, Haiyang Yu, Hongyu Lin, Yaojie Lu, Qiaoyu Tang, Fei Huang, Xianpei Han, Le Sun, and Yongbin Li. 2025. StructRAG: Boosting Knowledge Intensive Reasoning of LLMs via Inference-time Hybrid Information Structurization. In *The Thirteenth International Conference on Learning Representations*. https://openreview.net/forum?id=GhexuBLxbO

[30] Wanying Liang, Pasquale De Meo, Yong Tang, and Jia Zhu. 2024. A Survey of Multi-modal Knowledge Graphs: Technologies and Trends. *ACM Comput. Surv.* 56, 11, Article 273 (June 2024), 41 pages. doi:10.1145/3656579

[31] Aristidis Likas, Nikos Vlassis, and Jakob J. Verbeek. 2003. The global k-means clustering algorithm. *Pattern Recognition* 36, 2 (2003), 451–461. doi:10.1016/S0031-3203(02)00060-2 Biometrics.

[32] Weizhe Lin, Jinghong Chen, Jingbiao Mei, Alexandru Coca, and Bill Byrne. 2023. Fine-grained Late-interaction Multi-modal Retrieval for Retrieval Augmented Visual Question Answering. In *Advances in Neural Information Processing Systems*, A. Oh, T. Naumann, A. Globerson, K. Saenko, M. Hardt, and S. Levine (Eds.), Vol. 36. Curran Associates, Inc., 22820–22840. https://proceedings.neurips.cc/paper_files/paper/2023/file/47393e8594c82ce8fd83adc672cf9872-Paper-Conference.pdf

[33] Xin Lin, Changxing Ding, Jinquan Zeng, and Dacheng Tao. 2020. GPS-Net: Graph Property Sensing Network for Scene Graph Generation. In *Proceedings of the IEEE/CVF Conference on Computer Vision and Pattern Recognition (CVPR)*.

[34] Zihan Ling, Zhiyao Guo, Yixuan Huang, Yi An, Shuai Xiao, Jinsong Lan, Xiaoyong Zhu, and Bo Zheng. 2025. MMKB-RAG: A Multi-Modal Knowledge-Based Retrieval-Augmented Generation Framework. arXiv:2504.10074 [cs.AI] https://arxiv.org/abs/2504.10074

[35] Hanchao Liu, Wenyuan Xue, Yifei Chen, Dapeng Chen, Xiutian Zhao, Ke Wang, Liping Hou, Rongjun Li, and Wei Peng. 2024. A Survey on Hallucination in Large Vision-Language Models. *CoRR* abs/2402.00253 (2024). https://doi.org/10.48550/arXiv.2402.00253

[36] Junming Liu, Siyuan Meng, Yanting Gao, Song Mao, Pinlong Cai, Guohang Yan, Yirong Chen, Zilin Bian, Botian Shi, and Ding Wang. 2025. Aligning Vision to Language: Text-Free Multimodal Knowledge Graph Construction for Enhanced LLMs Reasoning. arXiv:2503.12972 [cs.CV] https://arxiv.org/abs/2503.12972

[37] Pei Liu, Xin Liu, Ruoyu Yao, Junming Liu, Siyuan Meng, Ding Wang, and Jun Ma. 2025. HM-RAG: Hierarchical Multi-Agent Multimodal Retrieval Augmented Generation. arXiv:2504.12330 [cs.CL] https://arxiv.org/abs/2504.12330

[38] Qi Liu, Yongyi He, Tong Xu, Defu Lian, Che Liu, Zhi Zheng, and Enhong Chen. 2024. UniMEL: A Unified Framework for Multimodal Entity Linking with Large Language Models. In *Proceedings of the 33rd ACM International Conference on Information and Knowledge Management* (Boise, ID, USA) *(CIKM '24)*. Association for Computing Machinery, New York, NY, USA, 1909–1919. doi:10.1145/3627673.3679793

[39] Xukai Liu, Ye Liu, Kai Zhang, Kehang Wang, Qi Liu, and Enhong Chen. 2024. OneNet: A Fine-Tuning Free Framework for Few-Shot Entity Linking via Large Language Model Prompting. *arXiv preprint arXiv:2410.07549* (2024).

[40] Pan Lu, Hritik Bansal, Tony Xia, Jiacheng Liu, Chunyuan Li, Hannaneh Hajishirzi, Hao Cheng, Kai-Wei Chang, Michel Galley, and Jianfeng Gao. 2023. Mathvista: Evaluating mathematical reasoning of foundation models in visual contexts. *arXiv preprint arXiv:2310.02255* (2023).

[41] Shiyin Lu, Yang Li, Qing-Guo Chen, Zhao Xu, Weihua Luo, Kaifu Zhang, and Han-Jia Ye. 2024. Ovis: Structural embedding alignment for multimodal large language model. *arXiv preprint arXiv:2405.20797* (2024).

[42] Yubo Ma, Yuhang Zang, Liangyu Chen, Meiqi Chen, Yizhu Jiao, Xinze Li, Xinyuan Lu, Ziyu Liu, Yan Ma, Xiaoyi Dong, et al. 2025. Mmlongbench-doc: Benchmarking long-context document understanding with visualizations. *Advances in Neural Information Processing Systems* 37 (2025), 95963–96010.

[43] Lang Mei, Siyu Mo, Zhihan Yang, and Chong Chen. 2025. A Survey of Multimodal Retrieval-Augmented Generation. arXiv:2504.08748 [cs.IR] https://arxiv.org/abs/2504.08748

[44] Boci Peng, Yun Zhu, Yongchao Liu, Xiaohe Bo, Haizhou Shi, Chuntao Hong, Yan Zhang, and Siliang Tang. 2024. Graph retrieval-augmented generation: A survey. *arXiv preprint arXiv:2408.08921* (2024).

[45] Stephen Roller, Emily Dinan, Naman Goyal, Da Ju, Mary Williamson, Yinhan Liu, Jing Xu, Myle Ott, Kurt Shuster, Eric Michael Smith, Y-Lan Boureau, and Jason Weston. 2020. Recipes for building an open-domain chatbot. *CoRR* abs/2004.13637 (2020). https://arxiv.org/abs/2004.13637

[46] Wei Shen, Yuhan Li, Yinan Liu, Jiawei Han, Jianyong Wang, and Xiaojie Yuan. 2023. Entity Linking Meets Deep Learning: Techniques and Solutions. *IEEE Transactions on Knowledge and Data Engineering* 35, 3 (2023), 2556–2578. doi:10.1109/TKDE.2021.3117715

[47] Wei Shen, Jianyong Wang, and Jiawei Han. 2015. Entity Linking with a Knowledge Base: Issues, Techniques, and Solutions. *IEEE Transactions on Knowledge and Data Engineering* 27, 2 (2015), 443–460. doi:10.1109/TKDE.2014.2327028

[48] Kristina P. Sinaga and Miin-Shen Yang. 2020. Unsupervised K-Means Clustering Algorithm. *IEEE Access* 8 (2020), 80716–80727. doi:10.1109/ACCESS.2020.2988796

[49] Shezheng Song, Shan Zhao, ChengYu Wang, Tianwei Yan, Shasha Li, Xiaoguang Mao, and Meng Wang. 2024. A Dual-Way Enhanced Framework from Text Matching Point of View for Multimodal Entity Linking. *Proceedings of the AAAI Conference on Artificial Intelligence* 38, 17 (Mar. 2024), 19008–19016. doi:10.1609/aaai.v38i17.29867

[50] Mohammed Suhail, Abhay Mittal, Behjat Siddiquie, Chris Broaddus, Jayan Eledath, Gerard Medioni, and Leonid Sigal. 2021. Energy-Based Learning for Scene Graph Generation. In *Proceedings of the IEEE/CVF Conference on Computer Vision and Pattern Recognition (CVPR)*. 13936–13945.

[51] Kaihua Tang, Yulei Niu, Jianqiang Huang, Jiaxin Shi, and Hanwang Zhang. 2020. Unbiased Scene Graph Generation From Biased Training. In *Proceedings of the IEEE/CVF Conference on Computer Vision and Pattern Recognition (CVPR)*.

[52] Qwen Team. 2024. Qwen2.5: A Party of Foundation Models. https://qwenlm.github.io/blog/qwen2.5/. Includes instruction-tuned Qwen2.5-72B-Instruct via Hugging Face.

[53] Vincent A Traag, Ludo Waltman, and Nees Jan Van Eck. 2019. From Louvain to Leiden: guaranteeing well-connected communities. *Scientific reports* 9, 1 (2019), 1–12.

[54] Yao-Hung Hubert Tsai, Shaojie Bai, Paul Pu Liang, J. Zico Kolter, Louis-Philippe Morency, and Ruslan Salakhutdinov. 2019. Multimodal Transformer for Unaligned Multimodal Language Sequences. In *Proceedings of the 57th Annual Meeting of the Association for Computational Linguistics*, Anna Korhonen, David Traum, and Lluís Màrquez (Eds.). Association for Computational Linguistics, Florence, Italy, 6558–6569. doi:10.18653/v1/P19-1656

[55] Ultralytics. 2023. Ultralytics YOLOv8: Cutting-Edge Object Detection Models. https://github.com/ultralytics/ultralytics. Accessed: 2025-07-14.

[56] Oriol Vinyals, Alexander Toshev, Samy Bengio, and Dumitru Erhan. 2015. Show and tell: A neural image caption generator. In *2015 IEEE Conference on Computer Vision and Pattern Recognition (CVPR)*. 3156–3164. doi:10.1109/CVPR.2015.7298935

[57] Bin Wang, Chao Xu, Xiaomeng Zhao, Linke Ouyang, Fan Wu, Zhiyuan Zhao, Rui Xu, Kaiwen Liu, Yuan Qu, Fukai Shang, et al. 2024. Mineru: An open-source solution for precise document content extraction. *arXiv preprint arXiv:2409.18839* (2024).

[58] Jingyi Wang, Jianzhong Ju, Jian Luan, and Zhidong Deng. 2025. LLaVA-SG: Leveraging Scene Graphs as Visual Semantic Expression in Vision-Language Models. In *ICASSP 2025 - 2025 IEEE International Conference on Acoustics, Speech and Signal Processing (ICASSP)*. 1–5. doi:10.1109/ICASSP49660.2025.10887586

[59] Peng Wang, Shuai Bai, Sinan Tan, Shijie Wang, Zhihao Fan, Jinze Bai, Keqin Chen, Xuejing Liu, Jialin Wang, Wenbin Ge, et al. 2024. Qwen2-vl: Enhancing vision-language model's perception of the world at any resolution. *arXiv preprint arXiv:2409.12191* (2024).

[60] Weiyun Wang, Zhe Chen, Wenhai Wang, Yue Cao, Yangzhou Liu, Zhangwei Gao, Jinguo Zhu, Xizhou Zhu, Lewei Lu, Yu Qiao, Jifeng Dai, and et al. 2024. InternVL2.5-MPO: Enhancing the Reasoning Ability of Multimodal Large Language Models via Mixed Preference Optimization. arXiv preprint arXiv:2411.10442.

[61] Thomas Wolf, Lysandre Debut, Victor Sanh, Julien Chaumond, Clement Delangue, Anthony Moi, Pierric Cistac, Tim Rault, Rémi Louf, Morgan Funtowicz, et al. 2020. Transformers: State-of-the-art natural language processing. In *Proceedings of the 2020 conference on empirical methods in natural language processing: system demonstrations*. 38–45.

[62] Peng Xia, Kangyu Zhu, Haoran Li, Tianze Wang, Weijia Shi, Sheng Wang, Linjun Zhang, James Zou, and Huaxiu Yao. 2025. MMed-RAG: Versatile Multimodal RAG System for Medical Vision Language Models. In *The Thirteenth International Conference on Learning Representations*. https://openreview.net/forum?id=s5epFPdIW6

[63] Danfei Xu, Yuke Zhu, Christopher B. Choy, and Li Fei-Fei. 2017. Scene Graph Generation by Iterative Message Passing. In *Proceedings of the IEEE Conference on Computer Vision and Pattern Recognition (CVPR)*.

[64] An Yang, Baosong Yang, Beichen Zhang, Binyuan Hui, Bo Zheng, Bowen Yu, Chengyuan Li, Dayiheng Liu, Fei Huang, Haoran Wei, et al. 2024. Qwen2. 5 technical report. *arXiv preprint arXiv:2412.15115* (2024).

[65] Barry Menglong Yao, Yu Chen, Qifan Wang, Sijia Wang, Minqian Liu, Zhiyang Xu, Licheng Yu, and Lifu Huang. 2023. AMELI: Enhancing Multimodal Entity Linking with Fine-Grained Attributes. *CoRR* abs/2305.14725 (2023). https://doi.org/10.48550/arXiv.2305.14725

[66] Chen Yin and Zixuan Zhang. 2024. A Study of Sentence Similarity Based on the All-minilm-l6-v2 Model With "Same Semantics, Different Structure" After Fine Tuning. In *2024 2nd International Conference on Image, Algorithms and Artificial Intelligence (ICIAAI 2024)*. Atlantis Press, 677–684.

[67] Shi Yu, Chaoyue Tang, Bokai Xu, Junbo Cui, Junhao Ran, Yukun Yan, Zhenghao Liu, Shuo Wang, Xu Han, Zhiyuan Liu, and Maosong Sun. 2024. VisRAG: Vision-based Retrieval-augmented Generation on Multi-modality Documents. *CoRR* abs/2410.10594 (2024). https://doi.org/10.48550/arXiv.2410.10594

[68] Rowan Zellers, Mark Yatskar, Sam Thomson, and Yejin Choi. 2018. Neural Motifs: Scene Graph Parsing With Global Context. In *Proceedings of the IEEE Conference on Computer Vision and Pattern Recognition (CVPR)*.

[69] Dun Zhang, Jiacheng Li, Ziyang Zeng, and Fulong Wang. 2024. Jasper and Stella: distillation of SOTA embedding models. *arXiv preprint arXiv:2412.19048* (2024).

[70] Fengzhi Zhao, Zhezhou Yu, Tao Wang, and Yi Lv. 2024. Image Captioning Based on Semantic Scenes. *Entropy* 26, 10 (2024). doi:10.3390/e26100876

[71] Chaofan Zheng, Xinyu Lyu, Lianli Gao, Bo Dai, and Jingkuan Song. 2023. Prototype-Based Embedding Network for Scene Graph Generation. In *Proceedings of the IEEE/CVF Conference on Computer Vision and Pattern Recognition (CVPR)*. 22783–22792.

[72] Shuyan Zhou, Shruti Rijhwani, John Wieting, Jaime Carbonell, and Graham Neubig. 2020. Improving candidate generation for low-resource cross-lingual entity linking. *Transactions of the Association for Computational Linguistics* 8 (2020), 109–124.

[73] Anni Zou, Wenhao Yu, Hongming Zhang, Kaixin Ma, Deng Cai, Zhuosheng Zhang, Hai Zhao, and Dong Yu. 2024. Docbench: A benchmark for evaluating llm-based document reading systems. *arXiv preprint arXiv:2407.10701* (2024).

MMGraphRAG: Bridging Vision and Language with Interpretable Multimodal Knowledge Graphs

Supplementary Material

A CMEL dataset

The CMEL dataset is a novel benchmark designed to facilitate the evaluation of Cross-Modal Entity Linking (CMEL) tasks, focusing on fine-grained cross-entity alignment in complex multimodal scenarios. It features greater entity diversity and relational complexity compared to existing datasets like MATE. The dataset comprises documents from three distinct domains—news, academia, and novels—ensuring broad domain diversity. Each sample includes a text-based knowledge graph (KG) derived from text chunks, an image-based KG created from per-image scene graphs, and the original PDF-format document. In total, the CMEL dataset includes 1,114 alignment instances, divided into 87 from news articles, 475 from academic papers, and 552 from novels. A more detailed introduction is conducted in Subsection A. Additionally, the dataset supports extensibility via a semi-automated construction pipeline, allowing for minimal human supervision to generate new samples. The construction process is introduced in Subsection B. And in Subsection C, the full experiment results on the CMEL dataset are presented.

A.1 A Detailed Introduction to the CMEL Dataset

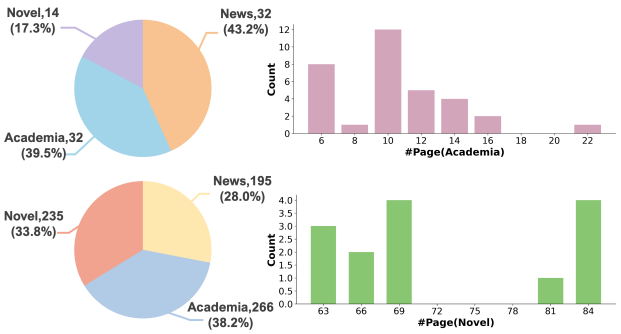

Figure 7: The Distribution of CMEL dataset. In the top-left, the number and proportion of documents in each domain are shown; in the bottom-left, the number and proportion of images in each domain are displayed; in the top-right, the page distribution of academia domain documents is provided; and in the bottom-right, the page distribution of novel documents is shown. All news domain documents are one page.

The distribution of dataset documents and images is shown in Figure 7. The entire dataset is constructed based on the number of images, so when divided by images, the number of documents in the three domains is approximately equal.

In addition to the text and image knowledge graphs, the CMEL dataset also contains a wealth of supplementary information to assist with the CMEL task. The text in the original documents is extracted into Markdown format using MinerU[57] and stored in the form of text chunks. The image information includes various details such as the corresponding text chunks and image descriptions, all summarized in a JSON file named `kv_store_image_data`. Take the entity corresponding to Figure 8 as a specific example.

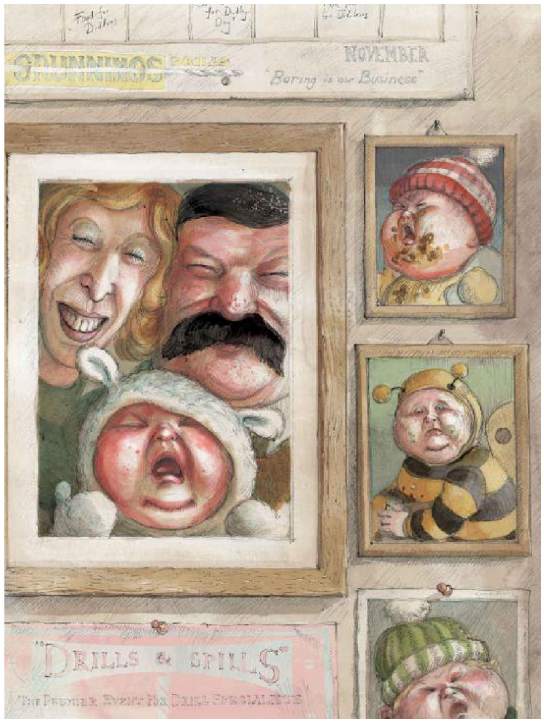

Figure 8: The Dursleys' photo wall. From Chapter 1 of "Harry Potter and the Sorcerer's Stone".

The original images are numbered starting from 1 in the order of their appearance and stored separately. The storage location can also be found in `kv_store_image_data`. Example data is as follows:

```
"image_2": {
        "image_id": 2,
        "image_path": "./images/image_2.jpg",
        "caption": [],
        "footnote": [],
        "context": "Mr. Dursley was the director of a
             firm called Grunnings...",
        "chunk_order_index": 0,
        "chunk_id": "chunk-
             fb8e5b95ca964e204d9e59caeaf25f09",
        "description": "The image depicts a wall adorned
             with framed pictures and posters. The
             central frame contains a family portrait
             featuring two adults and a baby...",
        "segmentation": true
    }
```

The ground truth for each instance is stored in a JSON file. Example data is as follows:

```
"image_2": [
        {
            "merged_entity_name": "BABY IN RED HAT",
            "entity_type": "PERSON",
            "description": "A small framed picture of a
                 baby wearing a red hat with a sad
                 expression...",
            "source_image_entities": [
                "BABY IN RED HAT"
            ],
            "source_text_entities": [
                "DUDLEY"
            ]
        },
       ...
    ]
```

The calculation formulas for the micro and macro accuracy in the CMEL dataset are as follows:

$$\text{Micro - Accuracy} = \frac{\sum_{i=1}^{N} \text{Correct}_i}{\sum_{i=1}^{N} \text{Total}_i} \tag{2}$$

Where N is the total number of entities. $Correct_i$ is the number of correct predictions for the ith image or entity, and $Total_i$ is the total number of predictions for the ith image or entity.

$$\text{Macro - Accuracy} = \frac{1}{M} \sum_{j=1}^{M} \frac{\text{Correct}_j}{\text{Total}_j} \tag{3}$$

Where M is the total number of documents. $Correct_j$ is the number of correct predictions for the jth document, and $Total_j$ is the total number of predictions for the jth document.

A.2 Construction of the CMEL Dataset

Step 0: Document Collection. The documents for the news and academia domains in the CMEL dataset are sourced from the DocBench dataset[73]. As for the novel domain, we choose several works especially suitable for the CMEL task. Specifically:

- In the academia domain, the papers come from arXiv, focusing on the top-k most cited papers in the natural language processing field on Google Scholar.
- In the news domain, the documents are collected from the front page scans of The New York Times, covering dates from February 22, 2022, to February 22, 2024.
- For the novel domain, four novels with a large number of images were downloaded from Zlibrary. To facilitate knowledge graph construction and manual inspection, these novels were split into 14 documents with approximately the same number of pages.

Step 1: Indexing. In this step, we follow the process introduced in Methodology to construct the initial knowledge graphs for the raw documents, including both text-based and image-based knowledge graphs. The specific operations are as follows:

- **Text-Based Knowledge Graph Construction:** First, text information is extracted from the raw PDF documents and chunked (fixed token sizes). Each text chunk is converted into a knowledge graph using LLMs, and stored in the file `kv_store_chunk_knowledge_graph.json`.
- **Image-Based Knowledge Graph Construction:** An independent image knowledge graph is constructed and stored in the file `kv_store_image_knowledge_graph.json`. Each image is linked to a scene graph, and its associated entity information, such as entity name, type, and description, is extracted and stored in the file `kv_store_image_data.json`.
- **Data Cleaning and Preparation:** Before storing the data, the working directory is cleaned, retaining only necessary files to ensure the cleanliness of the data storage.

Step 2: Check 1. In this step, LLM is used to determine whether there are any duplicate entities between different text chunks, assisting with manual inspection and corrections. The specific operations are as follows:

- **Adjacency Entities Extraction:** The `get_all_neighbors` function is used to extract adjacent entities associated with each text chunk to identify potential duplicate entities.
- **Entity Merge Prompt Generation:** Based on the content and entities of each text chunk, generate specific prompt. Then utilize LLM to determine whether these entities might be duplicates and provide suggestions for merging.
- **Manual Inspection:** The results from the LLM are manually reviewed to identify any duplicate entities and to edit the `merged_entities.json`, which serves as guides for the next step.

Step 3: Merging. After manual inspection, the entity merging phase begins, updating the entities and relations in the knowledge graph based on the confirmed results. The specific operations are as follows:

- **Entity Name Standardization:** All entity names are standardized to avoid matching issues caused by case differences.
- **De-duplication and Fusion:** The duplicate entities and relations are removed through the merge results, ensuring each entity appears only once in the graph, while updating the description of each merged entity.
- **Knowledge Graph Update:** The merged entities and relations are stored into the respective knowledge graphs, ensuring that the entities and relationships are unique and standardized.

The prompt for entity merging is as follows:

Prompt for Finding Duplicate Entities

You are an information processing expert tasked with determining whether multiple entities represent the same object and merging the results. Below are the steps for your task:

1.You will receive a passage of text, a list of entities extracted from the text, and each entity's corresponding type and description.

2.Your task is to determine, based on the entity names, types, descriptions, and their contextual relationships in the text, which entities actually refer to the same object.

3.If you identify two or more entities as referring to the same object, merge them into a unified entity record:

entity_name: Use the most common or universal name (if there are aliases, include them in parentheses). entity_type: Ensure category consistency. description: Combine the descriptions of all entities into a concise and accurate summary. source_entities: Include all entities that were merged into this entity record.

4.The output should contain only merged entities—entities that represent the same object and have been merged. Do not include any entity records for entities that were not merged.

-Input-

Passage:

A passage providing contextual information will be given here.

Entity List:

["entity_name": "Entity1", "entity_type": "Category1", "description": "Description1", "entity_name": "Entity2", "entity_type": "Category2", "description": "Description2", ...]

-Output-

["entity_name": "Unified Entity Name", "entity_type": "Unified Category", "description": "Combined Description", "source_entities": ["Entity1", "Entity2"],...]

-Considerations for Judgment-

1.Name Similarity: Whether the entity names are identical, commonly used aliases, or spelling variations.

2.Category Consistency: Whether the entity categories are consistent or highly related.

3.Description Relevance: Whether the entity descriptions refer to the same object (e.g., overlapping functions, features, or semantic meaning).

4.Contextual Relationships: Using the provided passage, determine whether the entities refer to the same object in context.

Step 4: Generation. In this step, LLM is used to generate the final alignment results, i.e., the alignment between image entities and text entities. The specific operations are as follows:

- **Image and Text Entity Alignment:** The LLM analyzes the entity information in the images and aligns it with the entities in the text chunks. The matching results for each image entity with the corresponding text entity are generated.
- **Generation of Final Results:** The generated alignment results are saved as `aligned_text_entity.json` files, ensuring that the entity information between the images and text is accurately aligned.

Step 5: Check 2. After generating the results, potential hallucination errors generated by the LLM (such as incorrect entity alignments) need to be screened and corrected. The specific operations are as follows:

- **Error Screening:** Check the alignment results generated by the LLM to identify any errors in the fused entity pairs. Ensure that entities requiring fusion actually exist.
- **Random Check:** A random sample comprising 20% of the data is manually reviewed to evaluate both the completeness and accuracy of the entity fusion process. Completeness refers to the proportion of entities that required fusion and were successfully merged, while accuracy pertains to the correctness of the merged entities. The results are shown in Table 5.

The prompt for fusion is as follows

Prompt for Entity Fusion

-Task-

Merge the text entities extracted from images and the entities extracted from nearby text (chunks). The two sets of entities should be merged based on context, avoiding duplication, and ensuring that each merged entity is derived from both image entities and text entities.

-Explanation-

1.Analyze the entities from the image and the entities from the nearby text, identifying which ones share overlapping or complementary context.

2.Merge entities only if there is a clear contextual link between them (e.g., they describe the same object, concept, or entity). Avoid creating a merged entity if it does not involve contributions from both sources.

3.For each pair of entities that are merged, output the unified entity name, category, the integrated description, and the original sources of the entities involved.

4.Discard entities that cannot be meaningfully merged (i.e., if no matching entity exists in the other source).

-Input Format-

Image Entities:

["entity_name": "Entity1", "entity_type": "Category1", "description": "Description1",

"entity_name": "Entity2", "entity_type": "Category2", "description": "Description2", ...]

Original Text:

[Here is a paragraph of text that provides context for the reasoning.]

Nearby Text Entities:

["entity_name": "Entity3", "entity_type": "Category3", "description": "Description3",

"entity_name": "Entity4", "entity_type": "Category4", "description": "Description4", ...]

-Output Format-

["entity_name": "Unified Entity Name", "entity_type": "Category", "description": "Integrated Description", "source_image_entities": ["Entity1"], "source_text_entities": ["Entity2"], ...]

The example provided in the prompt is intended to illustrate the task requirements and assist the LLM in understanding the specific objectives. And the example in the prompt is as follows:

```
-Example Input-
Image Entities:
[
{"entity_name": "Electric Sedan", "entity_type": "Product
     ", "description": "A high-end electric car focusing
     on performance and design"}
]

Original Text:
Tesla has a leading position in the global electric car
     market, with its Model S being a luxury electric
     vehicle equipped with advanced autonomous driving
     technology and excellent range.

Nearby Text Entities:
[
{"entity_name": "Tesla", "entity_type": "Company", "
     description": "A well-known American electric car
     manufacturer"},
{"entity_name": "Model S", "entity_type": "Product", "
     description": "A luxury electric vehicle released by
      Tesla"}
]

-Example Output-
{"merged_entity_name": "Model S", "entity_type": "Product
     ", "description": "Model S is a luxury electric
     vehicle released by Tesla, equipped with advanced
     autonomous driving technology and excellent range.",
      "source_image_entities": ["Electric Sedan"], "
     source_text_entities": ["Model S"]}
```

In this dataset, we are not concerned with the fusion results of the entities, but rather focus on whether the entities that need to be fused are correctly aligned. Therefore, it can also be said that we

are concerned with alignment. As a result, in this paper, we almost do not distinguish between the differences of fusion and alignment.

Performance	Type			Total.(196)
	News(26)	Aca.(61)	Nov.(109)	
Coverage	96.7	98.0	97.1	97.7
Accuracy	100	99.1	98.4	99.0

Table 5: Manual Inspection Results

A.3 Complete Results of the CMEL Dataset

In the fusion experiment, we selected different models for testing. The embedding-based similarity methods used three models: all-MiniLM-L6-v2[66] (MLM), bge-m3[8] (BGE), and stella-en-1.5B-v5[69] (Stella). For the LLMs, we chose Llama3.1-70B-Instruct[2] (L) and Qwen2.5-72B-Instruct[64] (Q), while for the MLLMs, we selected Qwen2-VL-72B[59] (Qvl) and InternVL2.5-38B-MPO[10] (Intvl).

For the clustering-based approach, the embedding model employed was uniformly Stella-EN-1.5B-V5. After clustering, CMEL requires selecting the appropriate cluster for the target image entity, with two specific methods: KNN[18] (K) and LLM-based judgment (L). The LLM utilized was Qwen2.5-72B-Instruct.

The displayed experimental results represent the best outcomes from three runs, and the full results are presented in Table 6.

Method	micro/macro Acc.			Overall.
	News	Aca.	Nov.	
Embedding Model-based Methods				
MLM	2.2/1.7	15.4/14.9	3.9/2.8	9.0/6.5
BGE	6.5/5.7	26.9/26.5	9.3/8.4	17.0/13.5
Stella	10.8/8.4	33.1/34.5	9.0/7.5	20.0/16.8
LLM-based Methods				
L-Qvl	10.8/8.4	33.1/34.5	9.0/7.5	20.0/16.8
L-Intvl	10.8/16.7	30.2/30.0	13.5/13.3	20.8/16.8
Q-Qvl	31.2/24.1	32.2/33.3	19.4/23.2	26.1/26.8
Q-Intvl	33.3/24.1	36.8/36.1	17.4/20.8	27.1/27.0
Clustering-based Methods				
DB-K	48.4/43.1	57.0/58.4	29.9/31.3	43.5/44.3
DB-L	53.8/45.9	60.8/58.3	29.9/34.2	45.2/46.1
KM-K	48.4/41.5	58.2/59.4	29.6/29.4	43.9/43.4
KM-L	50.5/40.6	60.7/57.7	29.6/30.5	45.2/43.0
PR-K	50.5/43.0	61.0/56.4	29.2/33.2	44.7/44.2
PR-L	51.6/44.4	59.7/56.8	29.1/35.2	44.1/45.5
Lei-K	50.5/42.1	66.7/64.3	30.4/37.2	47.7/47.9
Lei-L	54.8/44.7	60.5/55.5	29.4/30.6	44.8/43.6
Spe-K	57.5/50.9	70.1/66.1	31.0/39.8	49.7/55.1
Spe-L	**65.5/56.9**	**73.3/69.9**	**31.2/39.4**	**51.8/59.2**

Table 6: Complete Results for CMEL dataset

The performance differences across embedding models are quite pronounced: in particular, the relatively weak all-MiniLM-L6-v2 model nearly fails to achieve effective cross-modal entity alignment when using embedding-based similarity methods. The same pattern holds for LLM-based approaches: Llama 3.1-70B-Instruct performs significantly worse than Qwen 2.5-72B-Instruct in both the news and novel domains, indicating that CMEL task performance is heavily influenced by model architecture and capability. By contrast, clustering-based methods yield more consistent results on the CMEL task. Overall, assigning categories to image entities via LLMs outperforms KNN-based assignment, although the difference is modest. Moreover, the KNN approach requires one fewer model invocation and runs faster, so either method can be chosen flexibly depending on practical considerations and domain requirements.

B Complete Results of Multimodal DocQA Experiments

This experiment selects a variety of models as comparison benchmarks, including LLMs such as Llama3.1-70B-Instruct[2] (L), Qwen2.5-72B-Instruct[64] (Q), and Mistral-Large-Instruct-2411[3] (M), as well as MLLMs such as Ovis1.6-Gemma2-27B[41] (Ovis), Qwen2-VL-72B[59] (Qvl), and InternVL2.5-38B-MPO[10] (Intvl).

Model	Type					Domain			Overall Acc.
	Aca.	Fin.	Gov.	Laws	News	Text.	Multi.	Una.	
LLM-based Methods									
Llama	43.9	13.5	53.4	44.5	79.7	52.9	18.8	**81.5**	44.7
Qwen	41.3	16.3	50.7	49.7	77.3	53.9	20.1	75.8	44.8
Mistral	32.3	13.2	43.9	36.1	58.1	43.0	14.6	70.2	36.0
MMLLM-based Methods									
Ovis	16.2	11.1	23.6	25.7	39.0	22.8	8.8	54.8	21.3
Qvl	17.5	14.9	25.0	34.6	48.8	34.0	8.4	40.3	25.4
Intvl	19.8	16.3	28.4	31.4	46.5	35.7	15.9	39.5	27.7
NaiveRAG-based Methods									
Llama	43.6	38.2	66.2	64.9	**80.2**	79.9	32.1	70.2	61.0
Qwen	43.6	34.4	62.8	65.4	75.0	81.6	30.5	67.7	59.5
Mistral	44.9	35.4	58.1	62.3	76.7	76.5	32.1	69.4	58.6
GraphRAG-based Methods									
Llama	40.6	27.1	56.8	59.7	75.0	73.5	24.4	76.6	54.7
Qwen	39.6	25.7	52.5	49.7	74.5	71.7	26.0	67.5	52.3
Mistral	37.0	28.8	59.2	61.1	75.6	67.7	26.1	76.5	49.2
MMGraphRAG-based Methods (Ours)									
L-Ovis	49.7	43.6	58.5	60.0	75.3	75.1	62.5	76.3	64.1
Q-Ovis	50.3	46.4	59.4	56.1	76.8	76.3	63.4	74.2	65.3
M-Ovis	47.9	40.6	58.6	59.3	75.2	72.6	58.6	74.1	60.9
L-Qvl	51.8	59.4	62.8	60.7	77.9	79.1	77.8	70.2	74.0
Q-Qvl	51.8	62.9	**66.9**	68.6	76.2	**82.4**	81.1	67.7	75.2
M-Qvl	48.4	52.8	57.9	62.7	74.5	77.0	75.4	69.6	73.9
L-Intvl	**60.7**	64.1	62.6	64.9	76.2	80.0	86.4	75.0	**77.5**
Q-Intvl	60.5	**65.8**	66.5	**70.4**	77.1	81.2	**88.7**	71.9	76.8
M-Intvl	56.4	58.1	58.0	60.2	75.2	76.6	84.9	73.3	75.7

Table 7: Complete Results of DocBench Dataset. Based on the experimental results from a total of 21 combinations of the six models, designating Llama3.1-70B-Instruct as the evaluation model does not show undue favoritism towards its own generated results, thereby avoiding erroneous evaluation outcomes.

Among them, Ovis1.6-Gemma2-27B is deployed using the AutoModelForCausalLM from the Transformers[61] library, InternVL2.5-38B-MPO is deployed using lmdeploy[10], and the other models are deployed using vllm[26].

The complete results for the DocBench dataset are shown in Table 7, the complete results for the MMLongbench dataset are shown in Table 8, and the results for the MMLongBench dataset by domain are shown in Table 9.

Model	Locations			Modalities					Overall	
	Sin.	Mul.	Una.	Cha.	Tab.	Txt.	Lay.	Fig.	Acc.	F1
LLM-based Methods										
Llama	23.7	20.3	51.6	16.3	12.7	32.1	21.9	17.4	28.2	23.0
Qwen	22.5	20.0	53.2	16.8	12.6	33.3	23.5	16.1	27.8	22.1
Mistral	19.1	19.2	38.6	15.6	9.4	28.9	19.2	16.2	23.1	19.2
MMLLM-based Methods										
Ovis	10.6	9.5	13.0	6.9	3.1	10.0	15.4	15.4	10.7	9.2
Qvl	10.8	9.9	8.1	7.6	5.4	10.0	8.8	12.7	10.0	9.5
Intvl	13.3	7.9	13.9	8.8	8.1	10.7	11.8	11.4	11.6	10.4
NaiveRAG-based Methods										
Llama	24.9	19.5	56.5	16.3	15.3	31.0	22.7	18.7	29.2	24.2
Qwen	22.3	16.4	52.5	15.1	10.8	30.3	20.3	14.9	26.2	20.9
Mistral	21.6	19.2	52.9	15.4	12.5	31.2	20.6	13.7	27.3	22.8
GraphRAG-based Methods										
Llama	16.3	12.3	78.5	7.6	6.7	25.1	15.0	10.6	27.2	18.2
Qwen	18.2	13.2	77.1	14.0	11.0	26.1	12.2	8.5	28.1	19.3
Mistral	13.8	10.6	**86.5**	9.0	5.2	21.7	13.4	7.6	27.2	16.8
MMGraphRAG-based Methods (Ours)										
L-Ovis	36.9	13.0	57.4	24.4	23.7	26.8	15.9	24.1	31.0	26.8
Q-Ovis	37.4	15.5	54.4	24.9	23.3	28.0	26.1	27.6	31.6	27.5
M-Ovis	34.7	12.0	60.0	25.6	21.2	25.7	14.8	22.1	29.5	25.5
L-QVL	37.6	13.8	55.2	26.4	29.2	26.4	13.8	21.2	32.6	28.1
Q-Qvl	38.7	20.1	51.6	26.2	30.0	29.3	**29.1**	29.2	34.8	30.4
M-Qvl	36.4	12.1	56.8	27.6	27.7	23.2	11.8	19.8	31.7	26.9
L-Intvl	38.7	21.9	59.2	**34.7**	**36.6**	31.9	12.9	28.5	36.9	32.4
Q-Intvl	**39.6**	**26.7**	55.8	34.7	36.5	**33.8**	28.7	**34.6**	**38.8**	**34.1**
M-Intvl	37.7	19.5	63.2	35.0	33.5	28.0	13.6	27.6	35.7	31.8

Table 8: Complete Results of MMLongBench Dataset. The GraphRAG-based method has a similar accuracy to the NaiveRAG-based method, but the F1 score is much different. This is because GraphRAG performs better in answering the Una category questions, which are the questions that cannot be answered. Therefore, its overall performance is somewhat worse. The MMGraphRAG-based method significantly outperforms both in accuracy and F1 score, indicating that it can better answer general questions and achieves better overall results.

Through comparative experiments with other single-modal and multi-modal models under various methods, we found that Llama3.1-70B-Instruct is capable of maintaining a degree of independence and objectivity during the evaluation process. This suggests that its evaluation mechanism can effectively distinguish the generation results of different models without bias arising from its own model origin. Therefore, it can be concluded that the evaluation conclusions based on Llama3.1-70B-Instruct are relatively reliable and can provide fair and accurate assessment results in multi-model docment QA experiments.

Model	Evidence Locations							Overall	
	Int.	Tut.	Aca.	Gui.	Bro.	Adm.	Fin.	Acc.	F1
LLM-based Methods									
Llama	33.5	32.1	27.7	24.7	22.0	31.1	18.8	28.2	23.0
Qwen	31.5	31.8	25.4	30.3	26.5	**36.6**	9.6	27.8	22.1
Mistral	28.2	25.7	19.3	22.0	22.9	32.8	8.4	23.1	19.2
MMLLM-based Methods									
Ovis	7.4	20.4	10.9	7.3	16.5	14.3	4.3	10.7	9.2
Qvl	7.8	20.1	6.8	10.6	9.8	11.6	7.2	10.0	9.5
Intvl	11.3	19.1	10.4	8.9	14.4	13.3	6.0	11.6	10.4
NaiveRAG-based Methods									
Llama	34.0	31.0	30.0	29.4	23.0	29.6	18.4	29.2	24.2
Qwen	30.0	27.6	25.9	31.1	17.0	32.1	12.8	26.2	20.9
Mistral	32.6	24.7	24.5	32.5	18.7	34.0	17.6	27.3	22.8
GraphRAG-based Methods									
Llama	30.8	27.0	25.0	29.7	24.0	34.4	16.7	27.2	18.2
Qwen	34.6	21.8	24.8	29.2	27.0	36.2	18.9	28.1	19.3
Mistral	34.4	22.3	24.9	28.1	26.0	31.6	15.5	27.2	16.8
MMGraphRAG-based Methods (Ours)									
L-Ovis	35.7	32.9	30.2	41.7	27.1	24.6	26.7	31.0	26.8
Q-Ovis	36.4	**38.9**	29.4	39.3	32.2	30.2	30.1	31.6	27.5
M-Ovis	36.5	34.2	29.4	38.3	31.5	22.5	25.5	29.5	25.5
L-Qvl	36.5	32.9	27.1	41.3	26.3	28.4	34.0	32.6	28.1
Q-Qvl	37.2	38.8	26.3	39.5	31.6	35.8	38.0	34.8	30.4
M-Qvl	37.0	35.2	26.5	38.8	30.9	26.4	32.2	31.7	26.9
L-Intvl	42.4	34.0	**36.8**	**42.8**	28.9	26.0	36.2	36.9	32.4
Q-Intvl	**43.3**	36.5	35.2	40.0	**32.7**	33.5	**41.0**	**38.8**	**34.1**
M-Intvl	42.9	35.0	35.6	38.9	31.1	23.2	35.2	35.7	31.8

Table 9: MMLongBench Dataset Domain Results. The MMGraphRAG method achieves the best performance across all domains except for the Administration/Industry file category. Notably, it demonstrates the most significant improvements in the Guidebook and Financial report categories, which are characterized by a high volume of charts ,tables and figures. These enhancements are far more pronounced than those of other methods.

The MMLongBench dataset encompasses a diverse range of document domains. These domains include Research Reports/Introductions (Int.), which typically feature academic or industry-oriented analyses and background information; Tutorials/Workshops (Tut.), focusing on instructional content for skill development or knowledge dissemination; Academic Papers (Aca.), containing scholarly research and findings; Guidebooks (Gui.), offering practical information and advice for specific topics or activities; Brochures (Bro.), designed for promotional or informational purposes in a concise format; Administration/Industry Files (Adm.), covering official documents or industry-specific reports; and Financial Reports (Fin.), presenting financial data and analyses.

C Generation Module

Given that the current technology for MLLMs is still not fully mature, the Generation module employs a hybrid-generation approach that combines results from an LLM (text-only model) and an MLLM (capable of processing text, images, and other multi-modal information). This strategy aims to enhance the accuracy and stability of the final output.

This hybrid strategy not only makes full use of the maturity and advantages of LLMs in specific tasks, ensuring high quality semantic understanding and language expression, but also enriches the generated content by integrating multi-modal information. This approach effectively mitigates the limitations of current MLLMs while ensuring an overall improvement in the quality of the system's generation.

The Generation module achieves hybrid-generation through five steps: First, it extracts relevant information from the output of retrieval module and generates an initial textual response using LLM. Next, the MLLM is invoked to combine image and text information to generate a multimodal response, which is then merged with other multimodal reponses through an LLM. Finally, the generated textual response and multimodal response are integrated to output a comprehensive and consistent final result.

A specific example of an execution process is as follows, with the user's query and the generated answer provided:

question: "What is the highest F1 score achieved on the Chinese OntoNotes4.0 dataset, according to Table 10?"

answer: "The highest F1 score on the Chinese OntoNotes4.0 dataset is 84.67."

type: "multi-modal-t"

evidence: "The question requires identifying the maximum value in a single column, which is straightforward."

LLM Response:

The information cannot be obtained from the provided data tables.

MLLM Responses:

response 1

*To answer the question about the highest F1 score achieved on the Chinese OntoNotes 4.0 dataset, we will refer to the table labeled "Table 10" in the image provided. This table displays the effects of varying hyperparameters, specifically the alpha values, on the performance metrics of two datasets: Chinese OntoNotes 4.0 and English QuoRef. The table columns include alpha values ranging from 0.1 to 0.9 in increments of 0.1. For each alpha value, there are corresponding F1 scores for both Chinese OntoNotes 4.0 and English QuoRef datasets. Upon examining the "Chinese OntoNotes 4.0" column in the table, we notice the following F1 scores for each alpha value:- alpha = 0.1: F1 score = 80.13 - alpha = 0.2: F1 score = 81.17 - alpha = 0.3: F1 score = 84.22 - alpha = 0.4: F1 score = 84.52 - alpha = 0.5: F1 score = 84.47 - alpha = 0.6: F1 score = 84.67 (bolded, indicating the highest score) - alpha = 0.7: F1 score = 81.81 - alpha = 0.8: F1 score = 80.97 - alpha = 0.9: F1 score = 80.21 From this data, it is clear that the highest F1 score for the Chinese OntoNotes 4.0 dataset is **84.67**, which is achieved at an alpha value of 0.6. This score is highlighted in bold in the table, further confirming its significance as the peak performance metric for this specific dataset within the given range of alpha values.*

response 2

According to the table in image 12, the highest F1 score achieved on the Chinese OntoNotes 4.0 dataset is 84.67, which occurs at an alpha value of 0.6. This table illustrates the effects of hyperparameters on the performance metrics of the Chinese OntoNotes 4.0 and English QuoRef datasets, showing that the F1 score for Chinese OntoNotes 4.0 peaks at 84.67 when (alpha) is set to 0.6.

response 3

I'm sorry, but I cannot provide an analysis of the table in the image as it was not provided.

Merged MLLM Response:

The highest F1 score achieved on the Chinese OntoNotes 4.0 dataset is 84.67, which occurs at an alpha value of 0.6. This information is confirmed by the data in Table 10, which displays the effects of varying hyperparameters, specifically the alpha values, on the performance metrics of two datasets: Chinese OntoNotes 4.0 and English QuoRef.

Final Result:

The highest F1 score achieved on the Chinese OntoNotes 4.0 dataset, according to analysis of the information provided, is 84.67. This optimal F1 score occurs when the alpha value is set to 0.6.

The prompt for merging multimodal responses is as follows:

Prompt for Merging MLLM responses

The following is a list of responses generated by a multi-modal model based on the same user Query but different images. Please perform the following tasks:

-Analyze the Responses: Identify any contradictions, repetitions, or inconsistencies among the responses.

-Reasonably Determine: Decide which response best aligns with the user Query based on the provided information, ensuring that the determination is based on the relevance and accuracy of the information in the response rather than a majority consensus, as the correct answer may only pertain to a specific image and may not align with the majority.

-Provide a Unified Answer: Deliver a single, unified response that eliminates contradictions, resolves ambiguities, and accurately addresses the user Query.

Additionally, retain any highly relevant information from the responses that supports or complements the unified answer.

D Implementation of the Fusion Module

The pseudocode for the entire fusion process is as above, which provides a clearer understanding of the input and output of each step. The final step utilizes the fused MMKG to construct an entity vector database (vdb), which facilitates the retrieval stage.

imgdata (image data) and *chunks* (text chunks) are both results of preprocessing, stored in their respective JSON files. *imgdata* is used to store various information related to images, while *chunks* store the text chunks of the entire document. *tkg* (text-based knowledge graph) is the result of the text modality processing module txt2graph. It is stored in JSON files for each chunk and also as a complete GraphML file. Here, we do not make a specific distinction between them. *ikg* represents the image-based knowledge graph. First, *ikg* is obtained from the *image* and *imgdata*. Then, the formal first step is to align the entities in *tkg* and *ikg*, and save the alignment results as $list_a$. Entities to be fused are filtered out from *ikg*, and the remaining entities are enhanced using *chunks* (context) and relevant entities from *tkg*, resulting in the enhanced image-based knowledge graph ikg_e.

Next, we perform a detailed search in *tkg* to align the global entity of the image. This involves extracting relevant text segments from chunks that are semantically related to the whole image. Once the entity is identified, matching is performed in *tkg*. If aligned entity is found, only the relations of ikg_e will be updated to obtain ikg_u, which naturally achieves alignment during fusion. If no aligned entity is found in *tkg*, ikg_e will be updated by supplementing a new entity obtained from chunks to form ikg_u. Finally, *tkg* and ikg_u are fused based on the results of $list_a$ to obtain the final *mmkg* (multimodal knowledge graph).

Algorithm 1 Fusion

```
function FUSION(images)
    Initialize imgdata ← image_data.json
    Initialize tkg ← chunk_knowledge_graph.json
    Initialize chunks ← text_chunks.json
    for each image ∈ images do
        if mmkg exists then
            continue to next iteration
        end if
        ikg ← FIND(imgdata, image)
        list^a ← ALIGN(tkg, ikg)
        ikg_e ← ENHANCE(list^a, ikg, tkg, chunks)
        ikg_u ← UPDATE(ikg_e, tkg, image, chunks)
        mmkg ← MERGE(ikg_u, tkg, list^a)
    end for
    vdb ← mmkg
    return mmkg, vdb
end function
```

The second step, entity enhancement, is achieved using the reasoning capabilities of LLMs. Based on the context information, entities from *tkg* are used to supplement visual entities that do not have aligned counterparts. The prompt to enhance entities is as follows:

Prompt for Enhancing Image Entities

The goal is to enrich and expand the knowledge of the image entities listed in the img_entity_list based on the provided chunk_text.

The entity_type should remain unchanged, but you may modify the entity_name and description fields to provide more context and details based on the information in the chunk_text.

For each entry in the img_entity_list, the following actions should be performed:

1. Modify and enhance the entity_name if necessary.
2. Expand the description by integrating relevant details and insights from the chunk_text.
3. Include an original_name field to capture the original entity name before enhancement.

Ensure the final output is in valid JSON format, only including the list of enhanced entities without any additional text.

After generating candidate entities, LLM is used to align visual entities, with the specific prompt as follows:

Prompt for Generating Image Feature Block Description

You are an expert system designed to identify matching entities based on semantic similarity and context. Given the following inputs:

img_entity: The name of the image entity to be evaluated.

img_entity_description: A description of the image entity.

chunk_text: Text surrounding the image entity providing additional context.

possible_image_matched_entities: A list of possible matching entities. Each entity is represented as a dictionary with the following fields:

entity_name: The name of the possible entity.

entity_type: The type/category of the entity.

description: A detailed description of the entity.

additional_info: Additional relevant information about why choose this entity (such as similarity, reason generated by LLM, etc.).

-Task-

Using the information provided, determine whether the img_entity matches any of the entities in possible_image_matched_entities. Consider the following criteria:

1.Semantic Matching: Evaluate the semantic alignment between the img_entity and the possible matching entities, based on their names, descriptions, and types. Even without a similarity score, assess how well the img_entity matches the attributes of each possible entity.

2.Contextual Relevance: Use the chunk_text and img_entity_description to assess the contextual alignment between the img_entity and the possible entity.

-Output-

If a match is found, only return the entity_name of the best-matching entity.

If no match meets the criteria (e.g., low similarity or poor contextual fit), only output "no match".

Do not include any explanations, reasons, or additional information in the output.

E Implementation of the Img2Graph Module

Image Segmentation. The initial step involves subjecting the input image to segmentation, which entails parsing the image into regions that possess distinct semantic meanings (referred to as image feature blocks). This process is achieved through the image segmentation function in the YOLOv8[23] model. The segmentation outcomes provide a finer-grained representation of image information, thereby establishing the foundation for subsequent entity extraction and relation modeling. The granularity of segmentation significantly influences the precision of edge delineation within knowledge graphs.

Image Feature Block Description. Subsequently, the MLLM is employed to generate text descriptions for each image feature block derived from the segmentation results. The generation process of

the model is guided by carefully designed prompts, which enable it to produce accurate and semantically rich information. These text descriptions not only construct independent entities for the image modality but also provide a bridge for subsequent alignment with the text modality. Specific prompts are as follows:

Prompt for Generating Image Feature Block Description

You are a multi-modal model capable of processing image feature blocks and generating detailed descriptions.

Your task is to first determine the category of the given image feature block (object, organism, or person) and then extract the entity's features from it, providing a detailed description.

Note that the entity in the image feature block may not be complete, such as a half-body photo of a person or a partial image of an object.

- If the entity is an object, describe the object's features, including its name, color, shape, size, material, possible function, and other significant characteristics.

- If the entity is an organism, describe the features of this organism (animal or plant), including species, name, age, color, shape, size, posture, or structural characteristics.

- If the entity is a person, describe the person's features, including gender, skin color, hairstyle, clothing, facial expression, age, and posture.

All image feature blocks have a black background, so focus solely on the entity's characteristics, and do not mention "the background is black" in the output.

The example in the prompt is derived from the processing results illustrated in Methodology, and the example is as follows:

```
The category of this image feature block is 'person'. The
      entity features are as follows:
Person Features:
- Gender: Female
- Hairstyle: Long hair, light brown, naturally falling
     with some hair pinned with a clip
- Eyes: Blue, large and expressive
- Expression: Smiling, appears friendly and joyful
- Age: Appears to be a young woman
- Clothing: Wearing a white shirt with the sleeves rolled
      up, revealing the wrists; paired with blue overalls
     , with dark blue straps; light blue sneakers on her
     feet
- Accessories: Orange shoulder bag on her right shoulder;
      brown belt tied around the waist
- Holding: Holding a vintage-style camera with both hands
     , the camera is black and silver, with a large lens,
      appearing professional
Overall, the character gives off a youthful, lively vibe
     with a touch of artistic flair.
```

Entity and Relation Extraction from the Image. This step employs an MLLM, guided by prompts, to identify explicit relations (e.g., "girl — girl holding a camera — camera") and implicit relations (e.g., "boy — the boy and girl appear to be close, possibly friends or a couple — girl"). The extracted entities and relations provide structured information for the multimodal extension of the knowledge graph.

Compared to traditional scene graph generation methods, MLLM-based approaches excel at extracting entities and inferring both explicit and implicit relations by leveraging the semantic segmentation and reasoning abilities of MLLMs, resulting in high-precision and fine-grained scene graphs.

The prompt for extracting entity and relation from image is as follows:

Prompt for Visual Entity and Relation Extraction

Given a raw image, extract the entities from the image and generate detailed descriptions of these entities, while also identifying the relationships between the entities and generating descriptions of these relationships. Finally, output the result in a standardized JSON format. Note that the output should be in English.

-Steps-

1. Extract all entities from the image.

For each identified entity, extract the following information:

- Entity Name: The name of the entity

- Entity Type: Can be one of the following types: [{entity_types}]

- Entity Description: A comprehensive description of the entity's attributes and actions

- Format each entity as ("entity"{tuple_delimiter} Entity_Name {tuple_delimiter} Entity_Type {tuple_delimiter} Entity_Description

2. From the entities identified in Step 1, identify all pairs of (Source Entity, Target Entity) where the entities are clearly related.

For each related pair of entities, extract the following information:

- Source Entity: The name of the source entity, as identified in Step 1

- Target Entity: The name of the target entity, as identified in Step 1

- Relationship Description: Explain why the source entity and target entity are related

- Relationship Strength: A numerical score indicating the strength of the relationship between the source and target entities

Format each relationship as ("relationship" {tuple_delimiter} Source_Entity {tuple_delimiter} Target_Entity {tuple_delimiter} Relationship_Description {tuple_delimiter} Relationship_Strength)

3. Return the output as a list including all entities and relationships identified in Steps 1 and 2. Use {record_delimiter} as the list separator.

4. Upon completion, output {completion_delimiter}

The examples contained within the prompt are excessively lengthy. For illustrative purposes, only a small excerpt is presented here to demonstrate the format, as follows:

```
("entity"{tuple_delimiter}"Girl"{tuple_delimiter}"person"
     {tuple_delimiter}"Wearing glasses, dressed in black,
      holding white and blue objects, smiling at the
     camera."){record_delimiter}
("entity"{tuple_delimiter}"Headphones"{tuple_delimiter}"
     object"{tuple_delimiter}"White headphones on the
     girl's ears."){record_delimiter}
...
("relationship"{tuple_delimiter}"Girl"{tuple_delimiter}"
     Headphones"{tuple_delimiter}"The girl is wearing
     headphones."{tuple_delimiter}8){record_delimiter}
("relationship"{tuple_delimiter}"Girl"{tuple_delimiter}"
     Phone"{tuple_delimiter}"The girl is holding a phone
     in her hand."{tuple_delimiter}8){record_delimiter}
...
```

Alignment of Image Feature Blocks with Entities. Based on the extracted visual entities, the feature blocks generated by segmentation are aligned with their corresponding textual entities. This step is accomplished through the recognition and reasoning capabilities of the MLLM. For example, based on the semantic content of the textual entity, "Feature Block 2" is identified as the image of a "boy," and a relation is established in the knowledge graph. This alignment not only connects feature blocks to entities but also strengthens the association between modalities.

The prompt for aligning visual entities is as follows:

Prompt for Visual Entity Alignment

-Objective-

Given an image feature block and its name placeholder, along with entity-description pairs extracted from the original image, determine which entity the image feature block corresponds to and output the relationship with the entity. The output should be in English.

-Steps-

1. Based on the provided entity-description pairs, determine the entity corresponding to the image feature block and output the following information:

- Entity Name: The name of the entity corresponding to the image feature block

2. Output the relationship between the image feature block and the corresponding entity, and extract the following information:

- Image Feature Block Name: The name of the input image feature block

- Relationship Description: Describe the relationship between the entity and the image feature block, with the format "The image feature block Image Feature Block Name is a picture of Entity Name."

- Relationship Strength: A numerical score representing the strength of the relationship between the image feature block and the corresponding entity

Be sure to include the {record_delimiter} to signify the end of the relationship.

The examples saved in the prompt are as follows:

```
Example 1:
The image feature block is as shown above, and its name
     is "image_0_apple-0.jpg."
Entity-Description:
"Apple" - "A green apple, smooth surface, with a small
     stem."
"Book" - "Three stacked books, red cover, yellow inner
     pages."
Output:
("relationship"{tuple_delimiter}"Apple"{tuple_delimiter}"
     image_0_apple-0.jpg"{tuple_delimiter}"The image
     feature block image_0_apple-0.jpg is a picture of an
      apple."{tuple_delimiter}7){record_delimiter}
```

Global Entity Construction. Finally, a global entity is constructed for the entire image, serving as a global node in the knowledge graph. This node not only provides supplementary descriptions of the image's global information (e.g., "meet on the bridge") but also enhances the completeness of the knowledge graph through its connections to local entities. Through this step, the knowledge graph can provide multi-level information from global to local, further enhancing retrieval capabilities.

Received 20 February 2007; revised 12 March 2009; accepted 5 June 2009